U.S. DEPARTMENT OF
ENERGY

PNNL- 21693

Prepared for the U.S. Department of Energy
under Contract DE-AC05-76RL01830

High-Surface-Area Inorganic Membrane for Process Water Removal: Application to Ethanol Fuel Production

~~OFFICIAL USE ONLY~~

~~May be exempt from public release under the Freedom of Information Act (5 USC 552), exemption number(s) and category:~~

~~CRADA Exemption 3~~

~~**Department of Energy review required before public release.**~~

~~John Holladay/Pacifc Northwest National Lab~~
~~Reviewing Official (Name/Organization)~~

~~August 30, 2012~~
~~Date~~

~~Guidance Used (If Applicable)~~

W Liu
S Jones
R Xing

August 2012

Pacific Northwest
NATIONAL LABORATORY

Proudly Operated by Battelle Since 1965

~~OFFICIAL USE ONLY~~

PACIFIC NORTHWEST NATIONAL LABORATORY
operated by
BATTELLE
for the
UNITED STATES DEPARTMENT OF ENERGY
under Contract DE-AC05-76RL01830

Printed in the United States of America

Available to DOE and DOE contractors from
the Office of Scientific and Technical
Information,
P.O. Box 62, Oak Ridge, TN 37831-0062
www.osti.gov
ph: (865) 576-8401
fox: (865) 576-5728
email: reports@osti.gov

Available to the public from the National Technical Information Service
5301 Shawnee Rd., Alexandria, VA 22312
ph: (800) 553-NTIS (6847)
or (703) 605-6000
email: info@ntis.gov
Online ordering: http://www.ntis.gov

PNNL- 21693

High-Surface-Area Inorganic Membrane for Process Water Removal: Application to Ethanol Fuel Production

W Liu
S Jones
R Xing

August 2012

Prepared for
the U.S. Department of Energy
under Award # DE-FC36-04GO98014

Pacific Northwest National Laboratory
Richland, Washington 99352

~~Pages 1 through 4 in this report contain Protected CRADA Information~~

~~OFFICIAL USE ONLY~~

Abstract

This report summarizes process research results about concept development of a thin flat sheet water-selective molecular sieve membrane a breakthrough membrane product technology for separation of water from ethanol-enriched process streams. The studies include 1) membrane separation performance testing with real-world feeds sampled from the Pacific Ethanol Inc. ethanol plant at Boardman, Oregon, and 2) process design and simulation of membrane separation implementation into a corn ethanol plant. The separation tests were conducted on a laboratory-bench testing apparatus in a batch operation mode with small membrane samples (about 1-in. diameter) but under practical conditions, while the process simulation was performed using Aspen and U.S. Department of Agriculture models. A two-stage membrane separation system is proposed to conduct ethanol enrichment and purification by replacing respective distillation and adsorption processes. More than 90% energy saving can be obtained using the membrane separation. It is estimated that the membrane unit for a 40-million gal/year ethanol plant can be fairly compact, about the size of a plate heat exchanger due to high flux of the new membrane. The cost and lifetime of this new membrane product are critical factors to lower the capital cost. This membrane technology is promising for upgrading existing corn ethanol plants and for building of new cellulosic ethanol plants in the future as well. The results obtained in this work warrant further development of membrane module prototypes and demonstration of their long-term operation stability with slip streams at ethanol plants, which are necessary to move the technology toward commercialization.

Summary

A number of publications have been reported in the literature about using water-selective molecular sieve membranes for energy-efficient ethanol/water separation. However, almost all separation testing data reported in the literature were based on model ethanol/water mixtures, and no separation studies using real-world feedstock could be found prior to the start of this project. Furthermore, membrane pervaporation has often been stated (or claimed) as an energy-efficient separation technology in the literature reports, but no actual comparative process simulation was found in the literature prior to this work. This project fills these critical gaps for development of a new membrane product concept—thin flat sheet zeolite membranes. This membrane product may be produced via a roll-to-roll manufacturing process for mass production at a cost substantially lower than that for conventional zeolite membrane products.

Membrane separation performances were tested with feeds sampled from the Pacific Ethanol Inc. ethanol plant at Boardman, Oregon, on a laboratory-bench testing apparatus in a batch operation mode. Small membrane samples (only 1-in.-diameter) were used to minimize consumption of feeds and membrane materials, but testing was conducted under practical separation conditions. The membrane was quickly degraded using the as-received real feeds because the real feeds contained some acidic compounds that are detrimental to this type of zeolite membrane material. The stable membrane performances were shown by neutralizing the as-received feed with an alkaline hydroxide solution such as NaOH and KOH or by using a guide bed to scrub the acidic and other harmful species from the as-received feed prior to its contact with the zeolite membrane. It was discovered that a defective zeolite membrane may be cured under the separation conditions with a feed containing small amounts of NaOH or KOH. The membrane showed very high water permeation flux, compared to the previous literature reports.

Process design and simulation for implementation of membrane separation into a corn ethanol plant of 40 million gal/year production capacity was performed using Aspen (Aspen Technology, Inc., Burlington, Massachusetts) and U.S. Department of Agriculture models. Three design cases were studied, focused on using membrane separation for removal of water from the overhead of the beer column. A two-stage membrane pervaporation system is proposed to conduct ethanol enrichment and purification by replacing respective distillation and adsorption processes. In the pervaporation process, the overhead stream of the beer column is introduced into the feed side of the membrane, i.e., under the overhead conditions, while the permeate side of the membrane is maintained under vacuum to generate a positive partial pressure (or fugacity) gradient for water vapor to transport across the membrane. Thus, the membrane pervaporation completely eliminates the need for steam to drive the distillation and adsorption separation processes in current plants. Energy consumption of the existing separation processes is dominated by steam usage. As a result, more than 90% energy savings can be obtained using the membrane separation.

The membrane unit for a 40-million gal/year ethanol plant can be fairly compact due to high flux of the new membrane. Membrane module sizes in the two-stage membrane unit are estimated to be only 1.4 and 2.8 m^3, respectively. These sizes are small enough to be comparable to the size of industrial plate heat exchangers, suggesting that the membrane unit would require little plant space and involve low installation costs. For upgrading of existing corn ethanol plants, the major benefit lies in savings of steam usage, while membranes are the main cost item. For new plant construction, significant capital costs may

be saved in addition to the energy savings. The initial membrane cost and its lifetime are critical capital cost factors. The initial membrane cost may be reduced using a roll-to-roll manufacturing process that is enabled by current flat sheet membrane product designs, while the membrane lifetime has to be tested under practical operating conditions. Thus, next-stage project work to move the technology toward commercialization should be development of membrane module prototypes and demonstration of their long-term performances with slip streams at ethanol plants.

Acknowledgments

We thank our collaborators at Pacific Ethanol Inc. for their support of this project work: Mr. Paul Koehler, vice president of manufacturing; Mr. Lyndon Jones and Mr. Royce Todd, two ethanol plant managers; and Mr. Douglas Williamson, principal engineer. We also thank Dr. Tony Rao (a post doctor at PNNL) and Mr. Joshua Croshaw (a summer intern at PNNL) for carrying out some of membrane testing experiments, and colleagues at the Pacific Northwest National Laboratory, Dr. John Holladay, Dr. James White, and Mr. Don Stevens, for their help in startup of this project. This project was a subset of an overall project that was funded by the U.S. Department of Energy Advanced Manufacturing Office (formerly Industrial Technology Program office) under Grant Agreement DE-FC36-04GO98014.

Acronyms and Abbreviations

bar	a unit of pressure equal to one million (10^6) dynes per square centimeter
°C	degree(s) Centigrade
°F	degree(s) Fahrenheit
g	gram(s)
gal	gallon(s)
HPLC	high-performance liquid chromatography
HP	horsepower
hr	hour(s)
ICP/AES	inductively coupled plasma/atomic emission spectrometry
in	inch(es)
kg	kilogram(s)
kPa	kilopascal(s)
kW	kilowatt(s)
lb	pound(s)
L	liter(s)
m	meter(s)
mm	millimeter(s)
min	minute(s)
NaA	NaA-type zeolite
PEI	Pacific Ethanol, Inc.
PNNL	Pacific Northwest National Laboratory
ppm	part per million
psia	pounds per square inch absolute
SEM/EDS	scanning electron microscopy/energy dispersive spectroscopy
USDA	U.S. Department of Agriculture
wt%	weight percent

Contents

Figures

Tables

1.0 Introduction

This Cooperative Research and Development Agreement (CRADA) project is a subset of the High-Surface-Area Inorganic Membrane for Process Water Removal project. Background data and information on zeolite membrane technologies, design and preparation of current thin flat sheet zeolite membranes, and testing results with model mixtures are summarized in a final DOE report for public release (Liu 2012). The present report summarizes the membrane separation process research results specifically for application to ethanol fuel production, which includes separation testing with real-world feeds and process design simulation and economic analysis for implementation of the new membrane technology into ethanol plants.

Corn-based ethanol fuel is already a large industry in the United States; the current output is more than 10 billion gal/year. There is a large growth potential for cellulosic ethanol in the future. In addition, sugar cane-based ethanol is a large industry in Brazil and other countries. A water/ethanol mixture is typically produced by currently known conversion technologies, regardless of feedstock. Ethanol/water separation is an energy-intensive process with current technologies such as distillation and adsorption. Thus, removal of water from ethanol/water mixtures represents a single large-application opportunity for the novel water-selective zeolite membrane technology developed in this project.

A great number of research studies have been reported in the literature about using water-selective molecular sieve membranes for energy-efficient ethanol/water separation. The pertinent literature reviews can be found in recent publications from this research group (Zhang and Liu 2011; Liu et al. 2011; Liu and Canfield 2012). However, almost all separation testing data reported in the literature were based on model ethanol/water mixtures, and no separation studies using real-world feedstock could be found prior to the start of this project. Furthermore, membrane pervaporation has often been stated (or claimed) as an energy-efficient separation technology in the literature reports, but no actual comparative process simulation was found in the literature prior to this work. This project fills these critical gaps for development of a new membrane product concept—thin flat sheet zeolite membranes.

2.0 Existing Ethanol Plant Operation and Feedstock Used for Separation Testing

~~(The following content is Protected CRADA Information)~~

Feedstock used for membrane separation testing in this project was obtained from Pacific Ethanol’s ethanol plant at Boardman, Oregon. This plant was designed by Delta T and included Resistance Temperature Detector (RTD) pressure distillation. Most U.S. ethanol plants were designed by ICM, which uses vacuum distillation. The processing capacity of the Boardman plant is about 41,000 bushels of corn per day, producing 40 million gal/year of ethanol (design capacity was 35 million gal/year). On a daily basis, the plant produces sufficient outputs to fill 26 trucks of wet cake, 29 trucks of syrup, and 10 to 11 trucks of ethanol. The ethanol product is shipped to Portland for gasoline blend, and the residual (mostly fibers, proteins, and oils) is sold to the local market for cattle feed. The wet cake contains about 68 wt% water compared to the 40 wt% water in the corn.

The boiler is the largest piece of equipment in the plant. The boiler is fueled with natural gas from a local gas supply and is equipped with economizers. The tap water is purified by a reverse osmosis (RO) membrane (GE) and dearated before being fed to the boilers to produce steam. The steam produced is at about 325 °F (162.8 °C) and 100 psi. The steam is used in the distillation column reboilers, stream heaters, and the clean-in-place system. Steam condensate is fully recycled.

Corn kernels are ground and mixed with process water (one-third of the thin stillage), ammonia, and α-amylase (enzyme) in a slurry tank at 180 °F (82 °C) for 8–10 min. The slurry tank is mixed with a 75-HP agitator. The slurry contains34–37% solids, percentages higher than most dry mills which typically run at 31–32% solids. The slurry is pumped into a baffled cooker (liquefaction tank) and mixed with 235 °F (113 °C) water (25% from the slurry tank, 75% water) and additional enzyme. The liquefaction tank is operated at 185 °F (85 °C) for 2 hr; no additional heating or cooling is used. The enzyme breaks down the starch, and the slurry becomes more fluidic. The slurry then is cooled down to 95 °F (35 °C) in plate-and-frame exchangers and pumped into the fermentation reactor. Each exchanger has about 100 plates. There are six exchangers and some of them might be used for fermentor cooling.

The fermentation section consists of four reactors installed in parallel that enable continuous batch operation by alternating the cleaning, feeding, fermentation, and discharging steps. Two fermentors operate at a time; the third is emptying (2 hr to empty) while the fourth is being filled. Every 12 hr, one of the four fermentors is taken offline. A beer well is used to buffer the fermented broth.

The 18% solids yeast mixture is charged into the fermentation tank with the cooked corn slurry at the beginning. The fermentation reactor has a design capacity of about 380,000 gal and is typically filled to a volume of about 350,000 gal. The fermentation temperature is critical to the ethanol yield. The temperature is controlled by slow stirring with an internal mechanical mixer and constant external cooling (normally cooling water, but chillers are used in the summer). Each fermentor vessel is uninsulated and has a single 15-HP agitator and a sloped bottom (for ease of discharge). The fermentation broth is withdrawn at the bottom, cooled through a planar heat exchanger, and fed back to the reactor at the top. The circulation flow rate is about 5,000 gal/min so that the reactor fluid is exchanged every 2 hr. The fermentation time is about 42 to 44 hr. The fermentation temperature is controlled at 95 ± 2 °F (~35 °C).

Carbon dioxide is pumped out of the reactor by vacuum, and the entrained liquid is scrubbed with water on a packed bed prior to being discharged into air.

At the start of fermentation, the solids loading is 34–37%, with a pH of 5.8. After the fermentation, the solids loading is about 9–10%, pH is about 4.2–4.5, and the ethanol content is about 16–19% by volume. Sugar conversion at 97–99% is achieved.

The fermentation broth is sent to the beer well, and sulfuric acid is added to bring the pH to about 3.7 in order to keep the minerals in solution. The liquid stream is heated up to 216 °F (102 °C) by steam prior to being fed into the beer column. The beer column consists of 22 trays at the lower section and 5 trays at the upper section above the feed. The column diameter is reduced in the upper section. A small condenser is installed directly on the top of the column, and the noncondensable portion of the stream is sent to the scrubber. The beer column feed conditions are 216 °F (xxx °C) at 40 psia. At the top section, the temperature is 220°F (104°C) and pressure is 30 psia. At the bottom section, the temperature is 255 °F (125 °C) and pressure is 33psia. The ethanol content is less than 0.5% in the bottom discharge.

The very bottom of the beer column temperature is controlled at 285 °F (xxx °C) to drive off all the ethanol. The bottom's solid content is drawn from the very bottom of the beer column. Ethanol is further removed in a stripping column. The resulting slurry, substantially free of ethanol, is sent to first evaporator to remove some of the water. The resulting whole stillage is sent to a centrifuge to generate thin stillage and produce wet cake (60–75% water). The thin stillage is then sent to two more evaporators to produce water and concentrated syrup. Evaporator #1 operates at 171 °F, 5.91 psia; evaporator #2 operates at 136.12 °F, 2.42 psia; and evaporator #3 operates at 119.42 °F and 1.5 psia. The water evaporated from the three evaporators is condensed and reused in the slurry tank. The bottoms from the third effect are fed to the second effect, which produces the syrup. The first effect is heated by the exchanging heat with the rectifier overhead; the next two effects are heated by cascading vapor from one effect to the next.

The largest difference between the plant operation and the U.S. Department of Agriculture (USDA) dry milling model is that in the model, the beer column bottom stream is centrifuged, then dewatered in an evaporator, followed by drying of the wet cake. Based on the USDA model, evaporation drying of the bottom stream consumes about 30% of the plant energy.

The vapor-phase stream is withdrawn from the overhead of the beer column and fed into a 20-tray rectifier. In the rectifier, process conditions are 200–203 °F (93–95 °C) and 28.29 psia at the top, and 219–220 °F (103–104 °C) and 29.26 psia at the bottom. The bottom stream of the rectifier is sent back to the stripper column, while the overhead vapor stream is sent to the adsorption section for purification. The rectifier also has five possible side-stream draw ports to remove fuel oils. Fuel oils (typically higher alcohols or other oxygenated species) are about 0.5% of the whole and are recycled (to the beer column).

The stripper column is also 20 trays and operates at 239.3 °F (115 °C) and 29.6 psia at the top and about 25 °F (-3 °C) and 30.9 psia at the bottom. The vapor off the top of the stripper is fed to the bottom of the rectifier along with the beer column condensable overhead stream. The stripper bottom is water (no ethanol) that is recycled.

Two adsorbent beds loaded with 3 mm of 3A adsorbent beads are used for removal of residual water from the rectifier overhead stream. The adsorbent loading of each bed is about 12,000–15,000 lb. The adsorbent cost is about \$2.5/lb. The two beds are operated alternately for adsorption and regeneration with a cycle time of about 3min. The adsorption bed operation programming looks to be built into the software so that the adsorption and regeneration are conducted automatically.

The adsorption and regeneration conditions (temperature and pressure) are dynamic because of the periodic switching. Typically, adsorption is conducted by flowing down the rectifier overhead stream downwardly through the bed. The adsorption temperature is at 220 °F (104 °C); the upper and lower pressures are 23psia and 22psia, respectively. The regeneration is conducted by purging the saturated bed with about 20% of the purified ethanol stream under vacuum. The ethanol flows upward through the bed. The regeneration temperature is about 250 °F (121 °C). The upper and lower pressures of the bed are 2.0–1.87 and 2.5–3.2 psia, respectively. However, the temperature and pressure constantly vary during the regeneration process. The vacuum is generated by Eductor with steam. The resulting alcohol regeneration stream (about70%) is recycled back to the rectifier to recover ethanol.

Dry ethanol product from the molecular sieves is sent to an acid reduction tank (with what looks like demister internals) to flash off any entrained volatiles. The volatiles are further scrubbed in the CO_2

scrubber operating at 11.2 in. water. CO_2 is vented to the atmosphere, and any liquid collected is recycled. The de-acidified ethanol is sent to a day tank and from there mixed with a denaturant (up to 5% gasoline) and sent to product storage.

~~**(The above content is Protected CRADA Information)**~~

Six 20-L containers were used to collect samples from three process streams for laboratory separation testing usage. Sampling from the beer column overhead was not successful because the vapor-phase stream could not be condensed into the liquid phase. Instead, the bottom stream of the rectifier was sampled. Some basic information about the three process samples is listed in Table 1. PEI#4 and PEI#5 were mixed at a 1:1 ratio to simulate the overhead stream of the beer column. The liquid was analyzed by the standard high-performance liquid chromatography (HPLC) method at PNNL.

Table 1. Three types of feedstock obtained from ethanol plant.

Feed ID	Ethanol content		pH	Notes
	g/L	wt%		
PEI#1	143.8	14.7	4.6	Beer column feed, looks like corn soup. Stable suspension as no apparent sedimentation after being stored 1 week. A clear solution was obtained with a 0.2-µm pore syringe filter for HPLC analysis.
PEI #4	222.9	23.0	3.6	Bottom of the stripper column, lightly colored solution
PEI #5	755.5	93.6	5.3	Overhead of the rectifier, clear solution
PEI#4 and PEI#5		58.3	4.5	1:1 mixture of PEI#4 and PEI#5 to simulate overhead stream of the beer column

All these samples are acidic. The NaA-type membrane is not stable in such an acidic solution. The acidic compound in the feed can be either removed or neutralized to prevent the membrane from degradation. This will incur some process change along with introduction of the membrane separation unit. If a basic compound is added into the feed to lower its pH, Table 2 shows that only small amounts of base addition are needed to make the solution become basic. The material cost of the base addition is small, well less than $0.02/gal of feed.

Table 2. Amount of base addition into feed for pH adjustment.

Feed with base addition	pH	Base added, wppm	Cost *, cent/gal
PEI #5 + NaOH	7	6	8.72E-04
	8	9	1.29E-03
	9	11	1.67E-03
PEI #5 + NH_4OH	7	19	2.81E-03
	8	38	5.64E-03
	9	115	1.73E-02
PEI #5 + baking soda ($NaHCO_3$)	7	16	2.38E-03
	8	25	3.74E-03
	9	51	7.68E-03
PEI#4 + NaOH	7	300	4.51E-02
	8	312	4.70E-02
	9	323	4.86E-02
PEI#4 and PEI5 + NaOH	7	100	1.50E-02
	8	141	2.12E-02
	9	150	2.25E-02

*Assume cost of the base as $0.5/kg.

3.0 Membrane Separation Testing

Membrane sheets were cut into 1-in.- diameter coupons that were loaded into a stainless steel test cell and tested in a batch operation mode (Liu 2012). In the batch operation, a fresh liquid-phase feed was charged into a reservoir at the beginning, and the feed was continuously pumped into the feed side of a membrane cell under constant conditions (temperature, pressure, flow rate) and returned to the feed reservoir while water was removed from the permeate side of the test cell under vacuum. Thus, in the batch operation, water content in the feed decreased gradually as the testing progressed.

3.1 NaA Membrane Performances with Neutralized PEI Feeds

Two membrane samples, which were grown in the Parr autoclave reactor, were installed into two test cells and tested in parallel with respective neutralized PEI and model feed. Variations of flux, selectivity, and ethanol content with testing time are plotted in Figures 1 and 2 for membrane Cell #1 and #2, respectively.

Cell # 1 was started with a neutralized PEI feed at 158 °F (70 °C; Figure 1a). The water flux decreased with time as a result of decreased water content in the feed and decreased partial-pressure differential of water vapor across the membrane. After 4 days of testing, the selectivity factor was above 12,000, indicating that the membrane was intact. The ethanol content in the permeate was plotted to explicitly show the membrane separation function. The water content in the feed was about 750 g/L. In contrast, the permeate ethanol content was below 2 g/L. Dehydration of the feed was estimated based on the composition of the feed sampled under the testing conditions at the same time for collection of the permeate. There was significant fluctuation in the feed content analysis. The feed sampling procedure and HPLC analysis of the high ethanol content will need to be checked and standardized in the future.

Testing of the membrane Cell #1 continued at 183 °F (84 °C) by charging the feed tank with a fresh feed several times in 3 weeks. Figure 1b shows that the water flux is around 1 to 2 kg/m^2/hr, which is lower than the flux numbers obtained at 158 °F (70 °C). This is contrary to the theoretical projection and model testing results. In general, the flux is expected to increase with the separation temperature. This phenomenon might suggest a strong impact of the feed composition on separation mechanisms. The selectivity factors were very high, around 16,000 to 36,000, which confirmed integrity of the membrane. The permeate ethanol content was below 1.8 g/L, far less than that of the feed (745 to 790 g/L).

At the same separation temperature of 183 °F (84 °C), when the feed-side pressure was increased from 135 to 264 kPa, water flux was increased by two to three times, as shown in Figure 1c, while the selectivity factor remained very high. The permeate ethanol content was less than 1.1 g/L. These results show that the membrane is stable after 21 days of continuous testing with the neutralized PEI feed.

Performances of Test Cell #2 are shown in Figure 2. For this membrane, the testing was started with the model feed at 158 °F (70 °C; Figure 2a). The water permeation flux decreased with testing time, which was expected, while the ethanol content in the feed increased with testing time. This membrane did not show a selectivity factor as high as did membrane Cell #1. However, comparison of the ethanol content in the permeate and the feed clearly shows that the membrane was still water-selective.

The feed tank was charged a few times with a fresh feed, and the membrane testing continued at 183 °F (84 °C) for 3 weeks. Figure 2b shows that the water flux decreased after the separation temperature was raised from 158 °F to 183 °F (70 °C to 84 °C), which is again contrary to the common expectation. The membrane was still water-selective, as judged by the large difference in ethanol content between the feed and permeate.

Very interesting results were obtained after switching from the model feed to the neutralized PEI feed. By comparing plots in Figures 2b and 2c, one can see that under the same testing conditions, both water flux and selectivity factor are dramatically higher with the neutralized PEI feed than with the model feed. The results suggest that some defects on the membrane may be repaired in situ by adding some basic compound to the feed. This happened even after the membrane was tested for 18 days with the model feed. This discovery was further investigated.

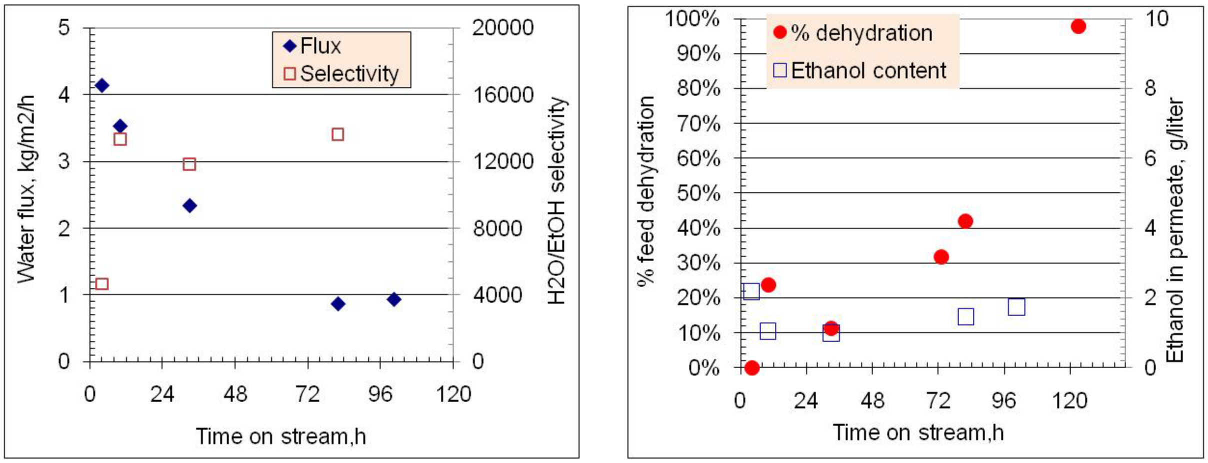

(a) Temperature: 70 °C; Feed-side Pressure: 135 kPa; Permeate-side Pressure: 3.6 kPa.

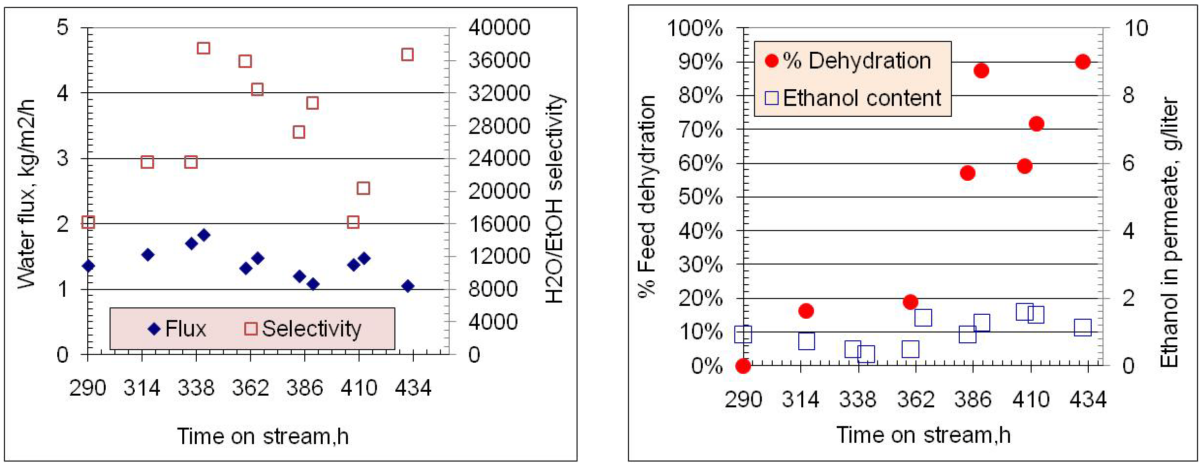

(b) Temperature: 84 °C; Feed-side Pressure: 135 kPa; Permeate-side Pressure: 3.6 kPa.

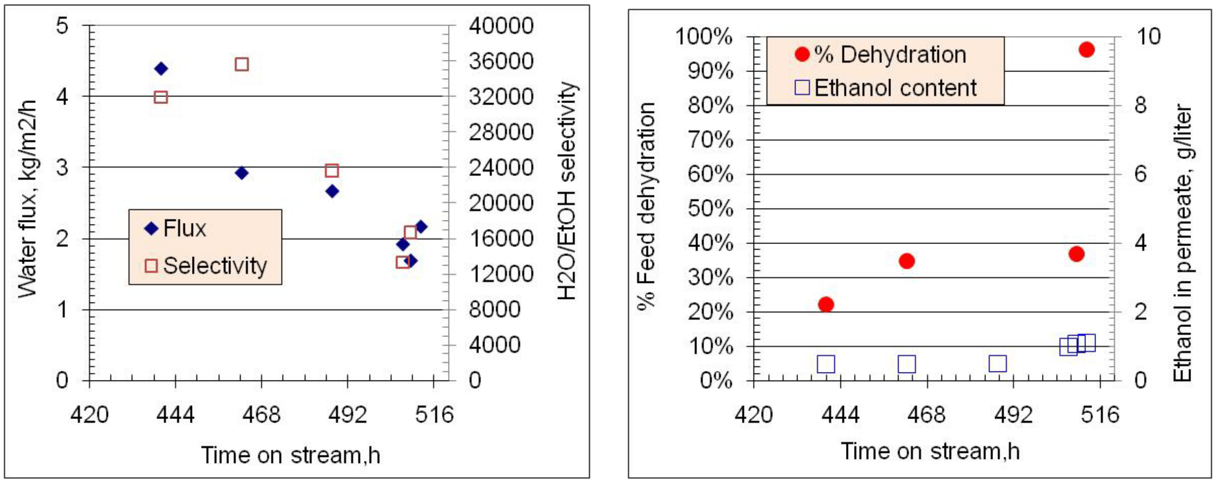

(c) Temperature: 84 °C; Feed-side Pressure: 264 kPa; Permeate-side Pressure: 3.6 kPa.

Figure 1. Long-term testing of membrane sample #1 (7710-2) with neutralized PEI#5.

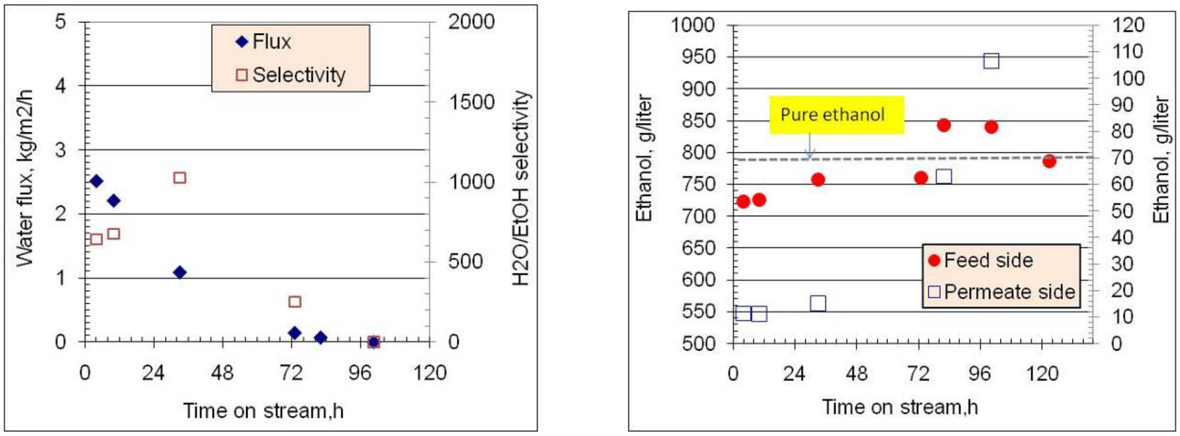

(a) Model feed; temperature of 70 °C; feed-side pressure 134 kPa; permeateside pressure 3.6 kPa.

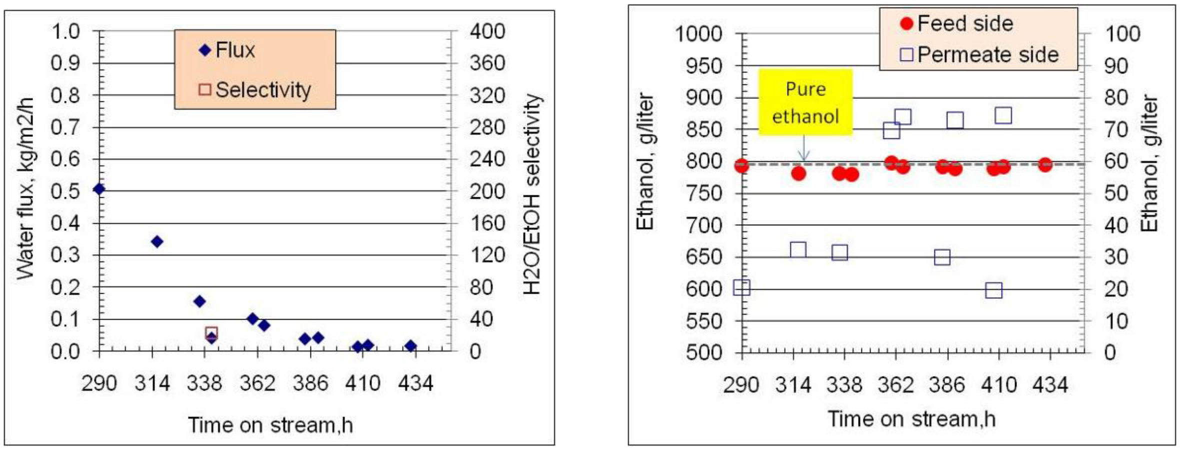

(b) Model feed; temperature 84 °C; feed-side pressure 134 kPa; permeate-side pressure 3.6 kPa.

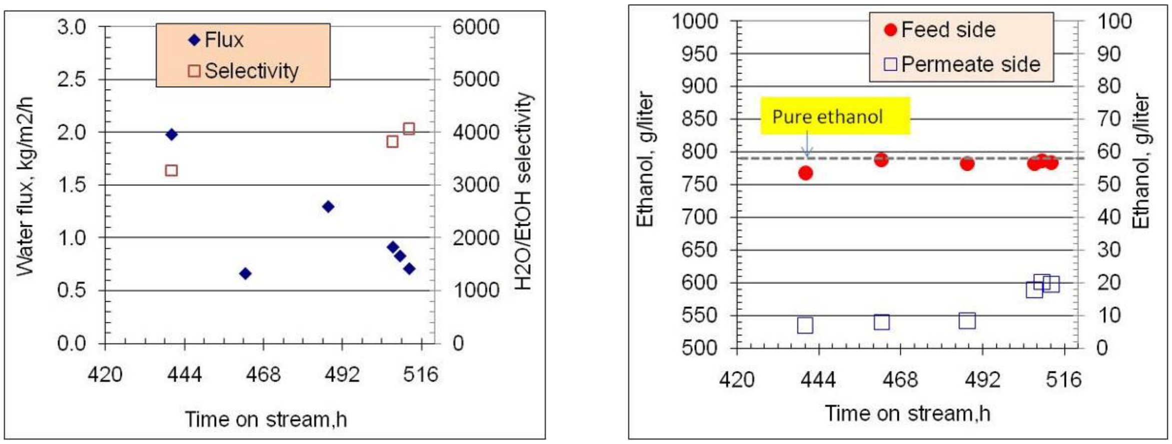

(c) Neutralized PEI#5; temperature 84 °C; Feed-side pressure 134 kPa; permeate-side pressure 3.6 kPa.

Figure 2. Long-term testing of membrane sample #2 (090110-2) at different temperatures with different feeds.

The testing results of two new membrane samples in 14 days of continuous run are summarized in Figure 3. Those two membranes were prepared under the same conditions in a Parr autoclave reactor except for stirring rate. Figures 3a and 3b compare impacts of NaOH addition into an ethanol/water mixture on the separation performance. The previous tests showed that neutralization of a real-world feedstock (PEI#5) by addition of NaOH dramatically enhanced the water permeation flux and H_2O/ethanol selectivity and also stabilized the membrane. However, addition of NaOH into a 90% ethanol/water model mixture did not show any improvement. To the contrary, the H_2O/ethanol selectivity factors without NaOH addition appear to be higher than those with NaOH addition. Plots in Figure 3b show that water permeation flux with the ethanol/water model feed declines with time. This is as expected because the water content in the feed continuously declined with testing time, and driving force for the water permeation was decreased. The water flux somehow increased with testing time in those plots of Figure 3a with the NaOH-added feed. The results suggest that addition of NaOH likely caused changes of the membrane structure under the separation conditions.

Effects of separation temperature on membrane performances are shown by plots in Figures 3b through 3d. The same model ethanol/water feed was used in these runs. There was no significant change in the membrane performance as the separation temperature was raised from 136 °F to 156 °F (58 °C to 69 °C). The feed was in the liquid phase, and the membrane separation occurred in the pervaporation mode. The water permeation flux and H_2O/ethanol selectivity increased as the temperature was raised to 203 °F (95 ^{o}C). At this temperature, the feed was likely in the gas phase and vapor-phase separation was taking place. These results are consistent with our previous observations.

At 203 °F (95 ^{o}C) of separation temperature, impacts of the feed on membrane performances are compared in Figures 3d through 3f. The water permeation flux was lower with the NaOH-neutralized PEI#5 than with the model ethanol/water feed. This may be due to lower water content in the PEI#5 feed. The H_2O/ethanol separation factors with the NaOH-neutralized PEI#5 are smaller than those with the model ethanol/water feed. The result reiterates the importance of conducting separation tests with real-world feeds. Membrane #2 shows higher water flux and selectivity than Membrane #1 for the NaOH-neutralized PEI#5. This indicates that the membrane quality may be affected by the reactor stirring rate (or mixing) during hydrothermal zeolite membrane growth. With a NH_4OH-neatralized PEI#5 feed, however, Membrane #2 rapidly lost its selectivity at this separation temperature, as evidenced by high ethanol content in the collected permeate. This phenomenon may be explained by vaporization of NH_4OH under the feed conditions.

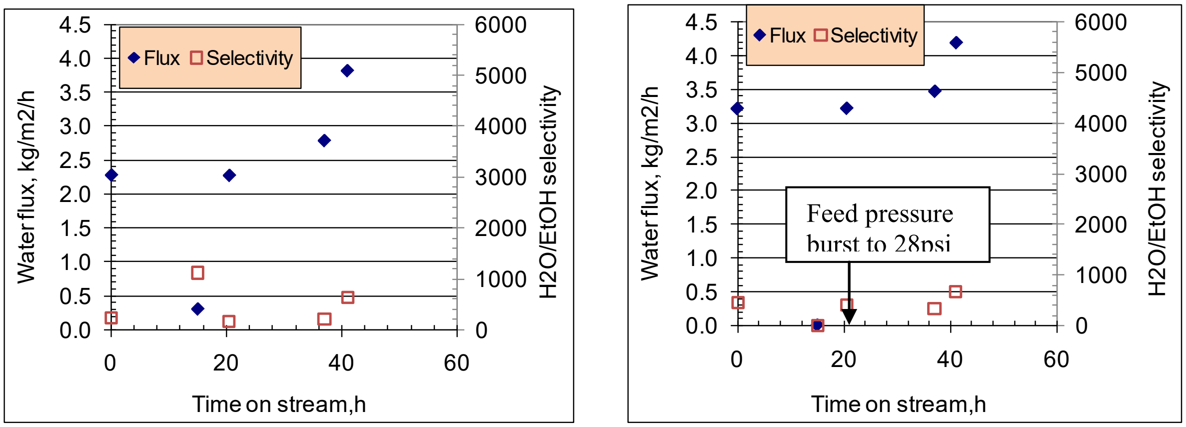

(a)-M#1 (55°C, 10psi, 90% ethanol @PH=8.5) (a)-M#2 (55°C, 10psi, 90% ethanol @PH=8.5)

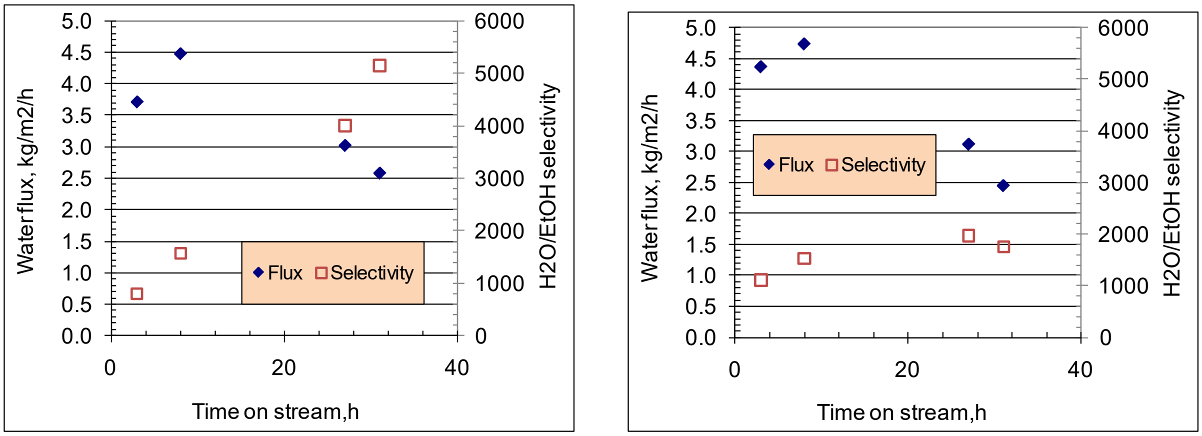

(b)-M#1 (58°C, 11psi, 90% ethanol @PH=6.6) (b)-M#2 (56°C, 10psi, 90% ethanol @PH=6.6)

Figure 3. Parametric tests of two NaA membrane samples in parallel (Mem#1 and #2 sampled from 2-in. x 4-in. membrane sheet grown on September 29 and September 28, 2010, respectively).

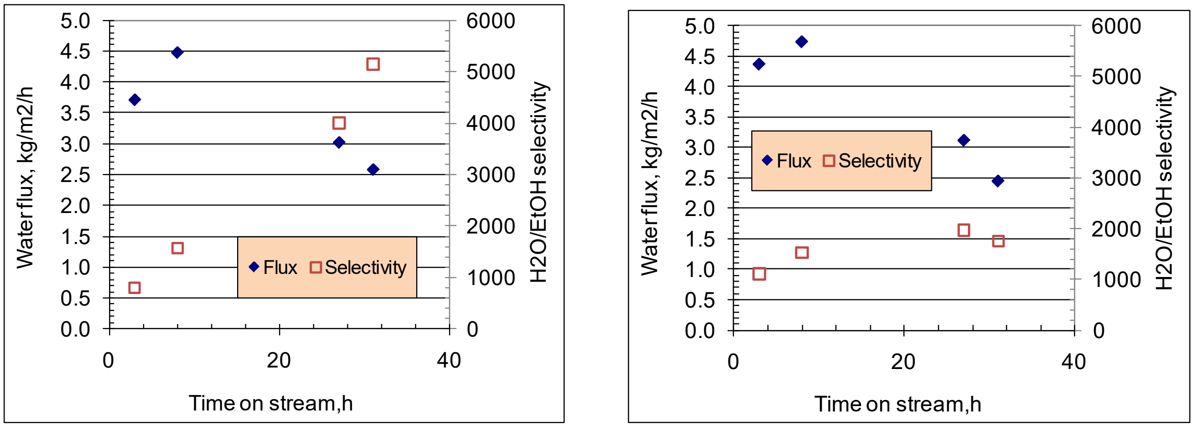

(b)-M#1(58^{o}C, 11psi, 90% ethanol/water)   (b)-M#2 (56^{o}C, 10psi, 90% ethanol/water)

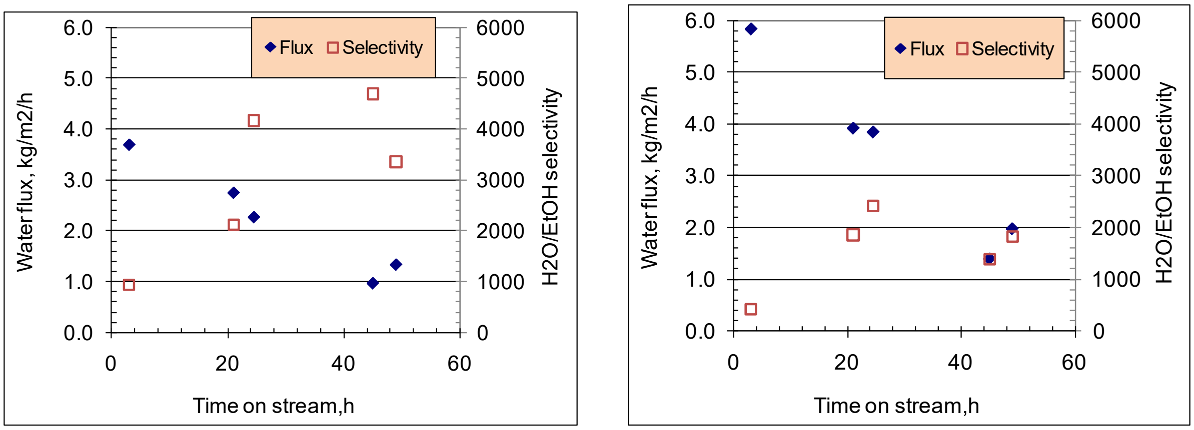

(c)-M#1 (69^{o}C, 15psi, 90% ethanol/water)   (c)-M#2 (68^{o}C, 15psi, 90% ethanol/water)

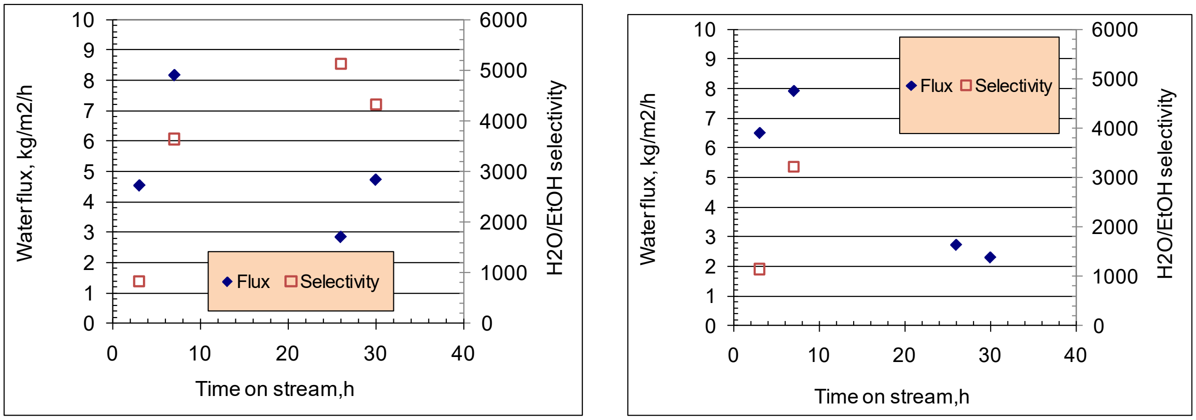

(d) M#1 (97^{o}C, 15psi, 90% ethanol/water)   (d) M#2 (95^{o}C, 14psi, 90% ethanol/water)

Figure 3. (contd)

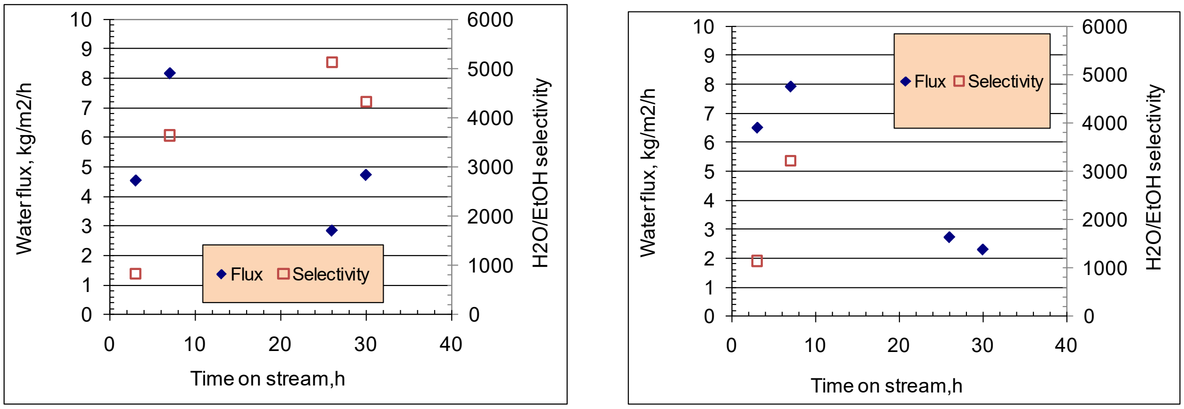

(d)-M#1 (97°C, 15psi, 90% ethanol @PH=7.1) (d)-M#2 (95°C, 14psi, 90% ethanol @PH=7.1)

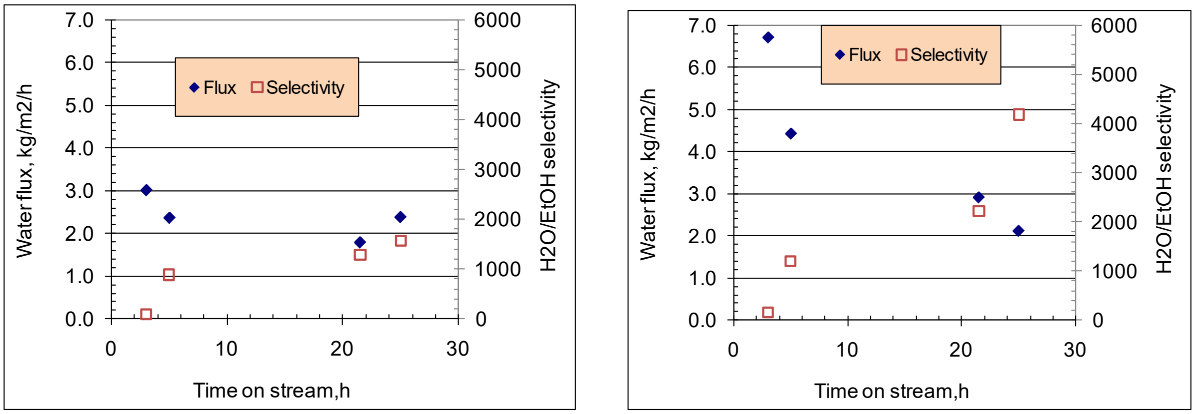

(e)-M#1 (95°C, 13psi, PEI#5 + NH_4OH @PH=8.5) (e)-M#2 (94°C, 14psi, PEI#5+NH_4OH@PH=8.5)

Membrane broken due to un-controlled start-up

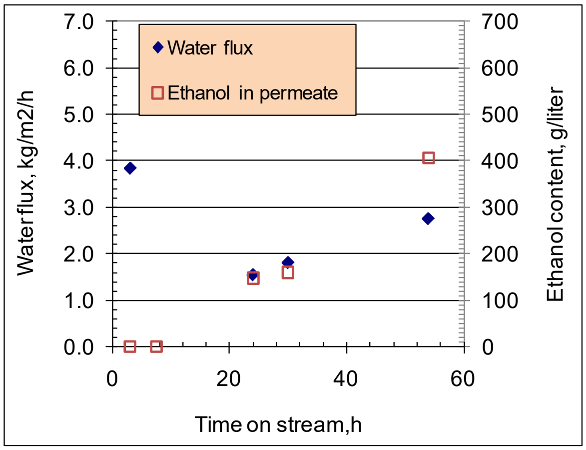

(f)-M#1 (95°C, 13psi, PEI#5 + NH4OH @PH=8.5) (f)-M#2 (94°C, 14psi, PEI#5 + NH4OH@PH=8.5)

Figure 3. (contd)

Membrane stability with the NH_4OH-neutralized PEI#5 feed was investigated further with new membrane cell loading. The membrane coupon was sampled from the same membrane sheet as Membrane #2 in runs shown in Figure 3 but from a different site. Figure 4 shows variations of the water flux and ethanol content in the permeate with time on stream. The time for the second batch run was begun with introduction of the newly charged feed into the membrane cell. In the first batch run, ethanol content in the permeate gradually increased with time. In the second batch run, the ethanol content in the permeate started from a high number (270 to 120 g/L) and rapidly increased with time. Such high ethanol content indicates that the membrane was no longer selective to water permeation. It is worth noting that the water flux was substantially lowered in the second batch. Thus, the porosity of the membrane was likely reduced concomitantly with the selectivity loss due to conversion of the zeolite crystal into an amorphous or glass phase. In conclusion, addition of NH_4OH into PEI#5 feed could not stabilize the NaA zeolite membrane at the separation temperature of 203 °F (95°C).

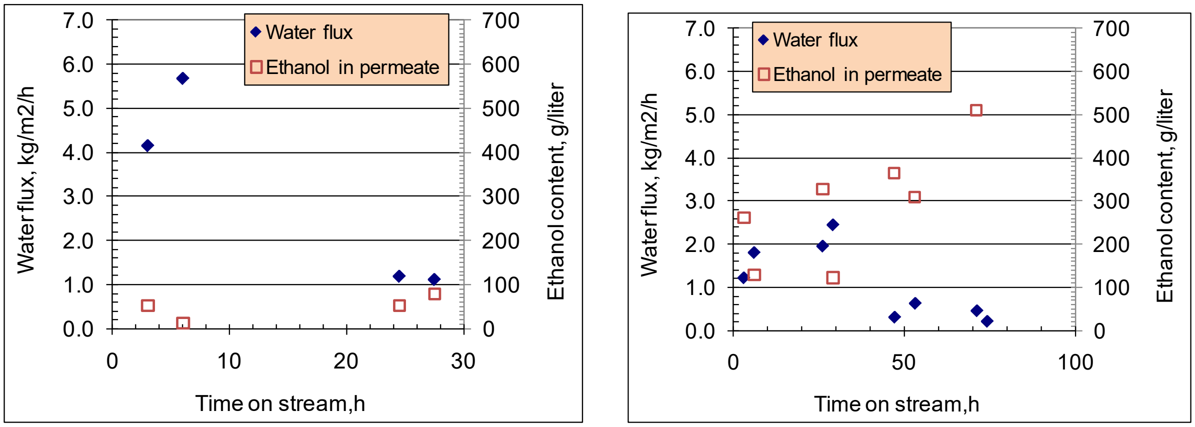

(a) First batch run (b) Second batch run

Figure 4. Membrane stability with NH_4OH-neutralized PEI#5 feed (Membrane #2 sampled from 2-in. x 4-in. membrane sheet grown on September 28, 2010; testing conditions: 95 °C, 15 psi, PEI#5 + NH_4OH @ pH = 8.5).

The impact on membrane stability of NaOH addition into the feed was tested further with new membrane loadings. Similar to the runs shown in Figure 3, Membranes #1 and #2 were tested in respective test cells in parallel. The results are summarized as plots in Figure 5. With the NaOH-added ethanol/water model feed (90% ethanol), both membranes maintained integrity at the separation temperature of 203 °F (95 °C), as evidenced by the decline of ethanol content in the permeate with time. This trend indicates that the NaOH addition may have made the membrane become more selective with time. Membrane #2 showed higher water flux and lower ethanol content than Membrane #1.

Thus, Membrane #2 has better membrane quality than Membrane #1, which is consistent with the conclusion drawn from the previous runs. Membrane #1 was broken during the feed switch. Testing of Membrane #2 was continued with the NaOH-added PEI#5 feed. The permeate ethanol content declined with time due to the stabilization effect of the NaOH addition. Then the feed was switched to a mixture of PEI#4 and PEI#5. The test cell temperature was lowered to 176 °F (80 °C) after the feed switch while the oven temperature was maintained the same. The cell temperature decrease caused by switching the feed under a constant oven temperature is believed resulting from a change in water vaporization of the feed. With the new feed, water permeation flux was nearly doubled due to higher water content in the feed. The ethanol content in the permeate was very low (less than 1 g/L), which means excellent membrane selectivity. These testing results confirm stabilization effects of NaOH addition into the feed.

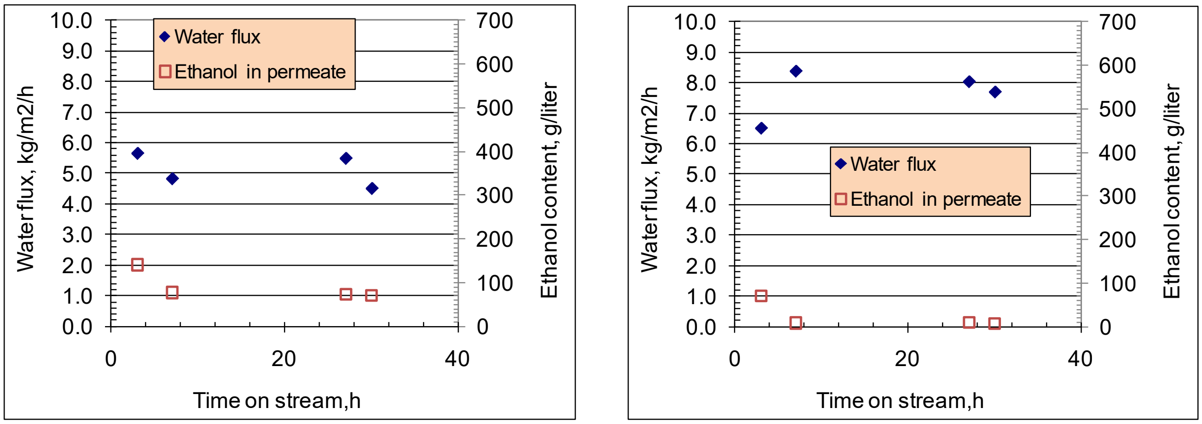

(a)-M#1 (96°C, 15psi, 90% ethanol @PH=8.5)

(a)-M#2(90°C, 14psi, 90% ethanol @PH=8.5)

Membrane broken during feed switch

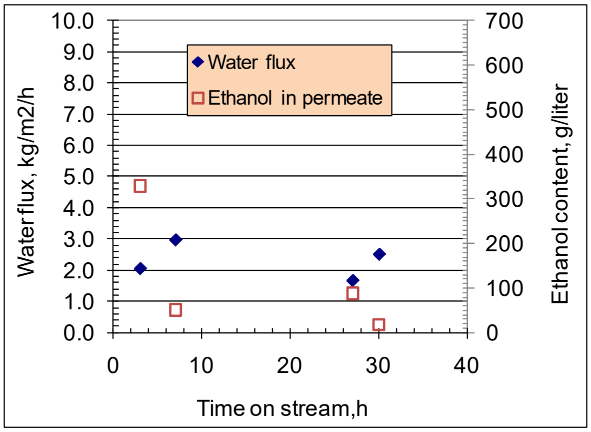

(b)-M#1 (95°C, 14psi, PEI#5 @PH=8.5)

(b)-M#2(95°C, 14psi, PEI#5 @PH=8.5)

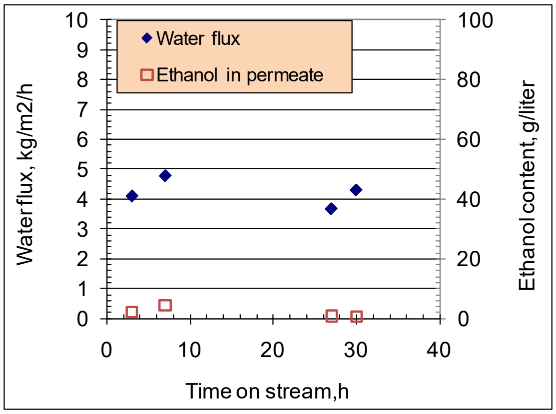

(c)-M#2(80°C, 14psi, PEI#5 and PEI#4 @PH=8.5)

Figure 5. Stability testing of two NaA membrane samples in parallel with different feeds (Membranes #1 and #2 sampled from 2-in. x 4-in. membrane sheet grown on September 29 and September 28, 2010, respectively).

3.2 NaA Membrane Stability Tests

Testing of the membrane sheets grown on September 28 and 29, 2010, was continued from the previous runs. Performances of those two membrane sheets, which were prepared under different stirring rates with the same procedure and conditions, are further compared in Figure 6. A model feed containing 90 wt% ethanol in water and neutralized with NaOH solution to pH = 8.5 was used. Under the similar separation conditions, Cell 1 shows much higher permeation flux and higher permeate ethanol content than Cell 2. For a given feed, ethanol content in the permeate reflects selectivity. The higher the ethanol content in the permeate, the lower the ethanol/water selectivity is. The results suggest that the membrane sample in Cell 2 may have fewer defects than the membrane in Cell 1. The stirring rate of the Parr reactor during membrane growth affects the membrane quality.

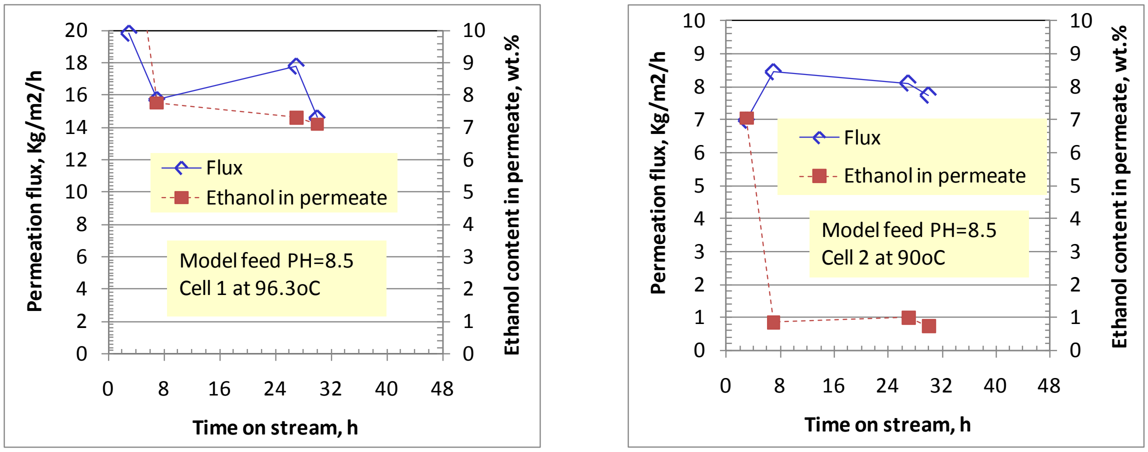

(a) Cell 1: membrane sheet 09/29/10 No.1 (b) Cell 2: membrane sheet 09/28/10 No.1

Figure 6. Comparison of membrane sheets grown under different stirring rates.

The membrane in Cell 1was accidently broken during the run, and testing of Cell 2 was continued. Figure 7 shows the impacts of feedstock on separation performances of Cell 2. The three feeds all were neutralized to pH = 8.5. However, they have different ethanol content and compositions. Under similar separation conditions, the permeation flux and permeate ethanol content are significantly affected by the type of feed. High permeation flux and ethanol/water selectivity are shown with the neutralized mixture of PEI#4 and PEI#5. Because the separation testing was run in the order of 1) model feed, 2) PEI#5, and 3) mixture of PEI#4 and PEI#5, the current results suggest that the membrane quality was improved with testing time.

Impacts of testing temperature on separation performances are shown in Figure 8. With the same neutralized mixture of PEI#4 and PEI#5, the permeation flux increases substantially by raising the separation temperature. The permeation flux at 206 °F (97 °C) is around 20 kg/m^2/hr and appears to be exceptionally high, relative to the dehydration membranes known from the literature, while permeate ethanol content is well below 0.2 wt%. The results indicate excellent performance of this membrane with the neutralized real-world feedstock.

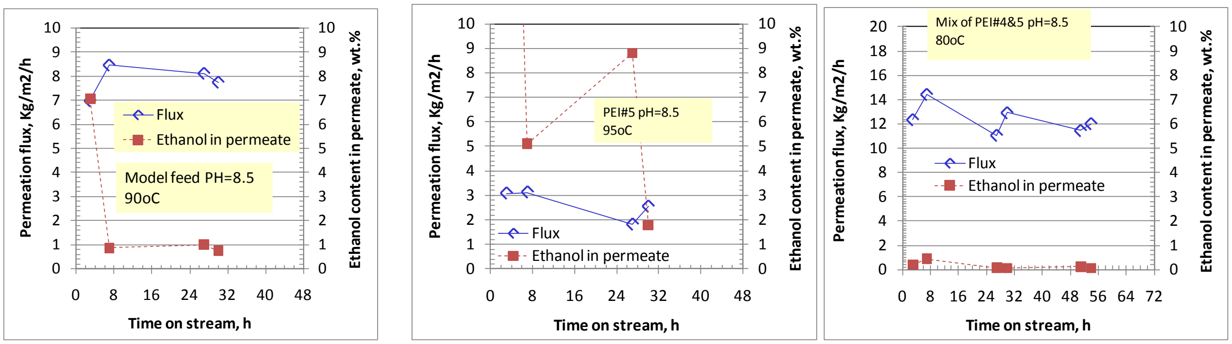

(a). Model feed (b) PEI#5 feed (c) Mix of PEI#4 and PEI#5

Figure 7. Impacts of feedstock on separation performances (Cell 2: membrane sheet 09/28/10 No.1 sheet).

Given the excellent performances, the membrane was tested with two more consecutive charges of the same feed but with a different base addition. NaOH was used for the former, while KOH was used for the latter. The results are shown in Figure 9. The permeation flux tended to decline with repeated runs. However, the membrane performance appeared to not reach a steady state within 2–3 days of testing after each charge of new feed. This is evidenced by the continuing increase of permeation flux and decrease of permeate ethanol content. In the batch-testing mode, ethanol content in the feed continuously declines as the separation testingproceeds. If the membrane property does not change, the permeation flux would decline with time due to decreased separation driving force—the partial pressure gradient of ethanol between feed and permeate.

Due to the outstanding performance of this membrane with the neutralized real feed, separation testing was continued with as-prepared feed, i.e., no base was added. As a result, the mixture of PEI#4 and PEI#5 becomes acidic with pH = 4.47. Figure 10 shows testing results of this membrane with three consecutive charges of the as-prepared feed. The permeation flux declines with time, while permeate ethanol content stays at a low level, < 1 wt%. Two trends are observed. One is that the permeation flux is lowered with each new feed charge. The second is that the permeate ethanol content becomes higher with each new feed charge. The trends indicate that gradual degradation of the membrane could be occurring.

Ethanol concentration in these batch runs is clearly illustrated by plots in Figure 11, which were derived from the same run as shown in Figure 10c. The ethanol content in the feed increases with time, while the ethanol content in the permeate stays at a low level. Ethanol was enriched from 57 wt% at the beginning to about 96 wt% in the end. After 40 days of testing, the membrane was unloaded from the testing cell and analyzed. The optical picture in Figure 12 shows deposition of white-colored materials on the membrane. Scanning electron microscopy (SEM) analysis shows the presence of amorphous phases and needle-like crystals, which are not zeolite crystals. Elemental analysis by energy dispersive spectroscopy (EDS) reveals significant presence of S and Ca elements. Thus, the surface deposit is likely due to formation of sulphate salts.

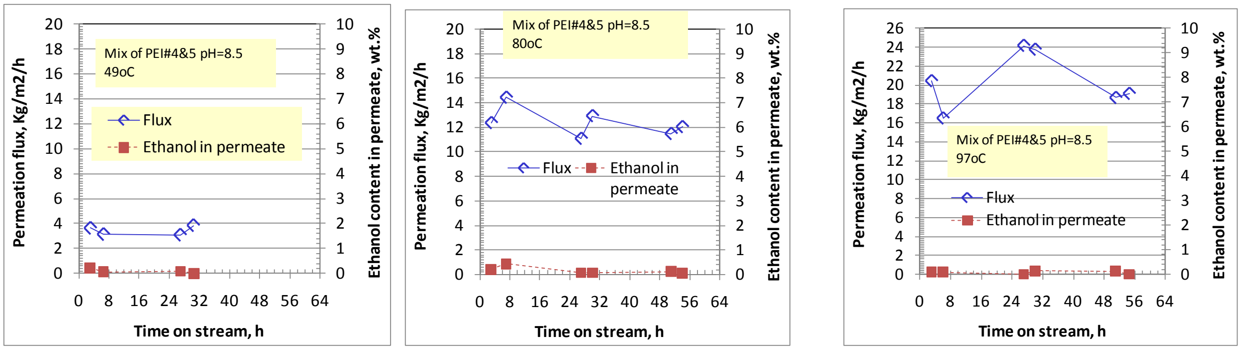

(a) 49 °C (b) 80 °C (c) 97 °C

Figure 8. Impacts of temperature on separation performances with neutralized mixture of PEI#4 and PEI#5 (Cell 2 membrane sheet 09/28/10 No. 1 sheet).

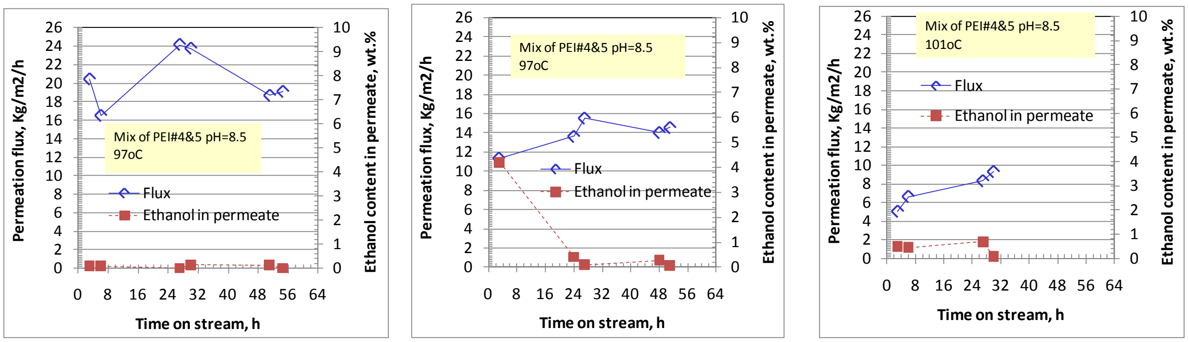

(a) First feed charge (b) Second feed charge (c) Third feed charge

Figure 9. Stability assessment of membrane separation performances at temperatures around 97 to 101 °C with neutralized mixture of PEI#4 and PEI#5 (Cell 2: membrane sheet 09/28/10 No.1 sheet).

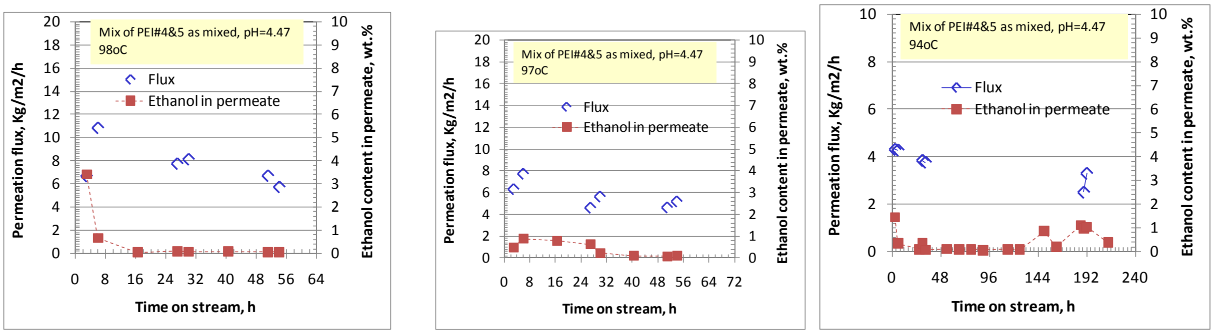

(a) First feed charge (b) Second feed charge (c) Third feed charge

Figure 10. Membrane separation performances with mixture of PEI#4 and PEI#5 as prepared (Cell 2: membrane sheet 09/28/10 No.1 sheet).

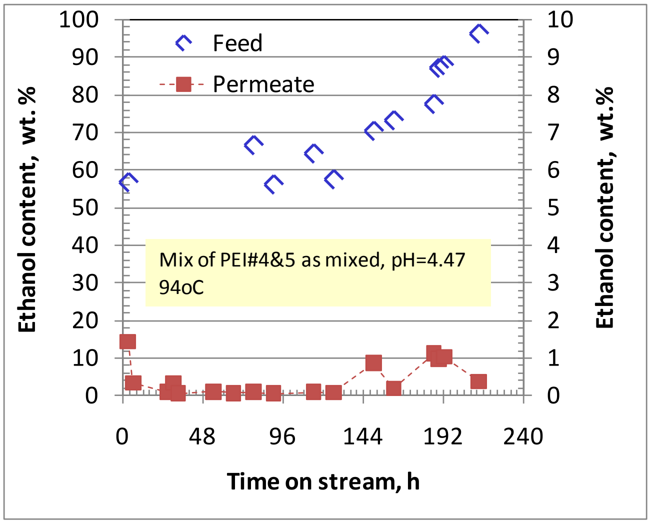

Figure 11. Concentration of ethanol in mixture of PEI#4 and PEI#5 with time on-stream (third charge shown in Figure 10; Cell 2: membrane sheet 09/28/10 No.1 sheet).

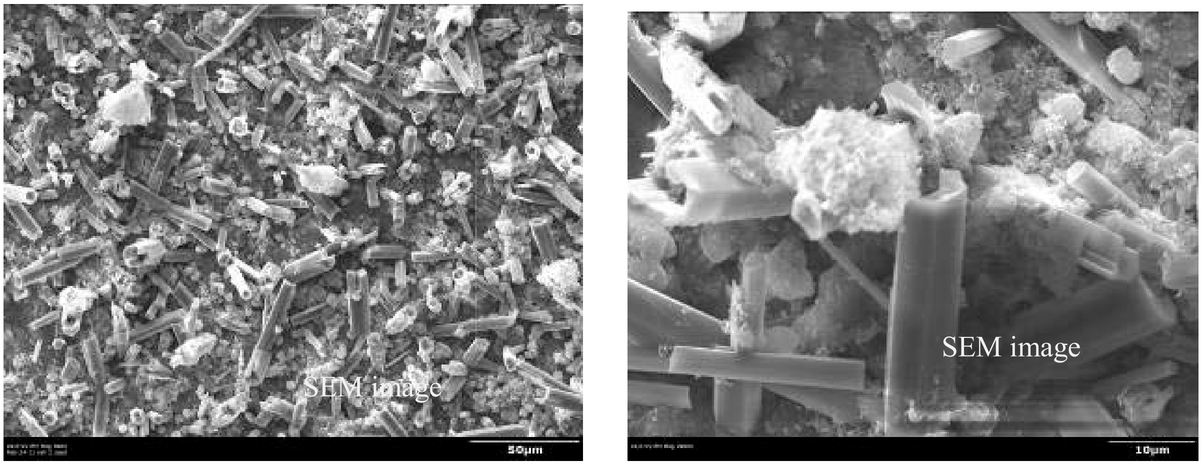

Elemental metal analysis of spent membrane surface

O	50.7
Na	0.42
Al	0.32
Si	0.14
S	25.2
Ca	22.1
Ni	0.82
Pd	0.3
Total	100

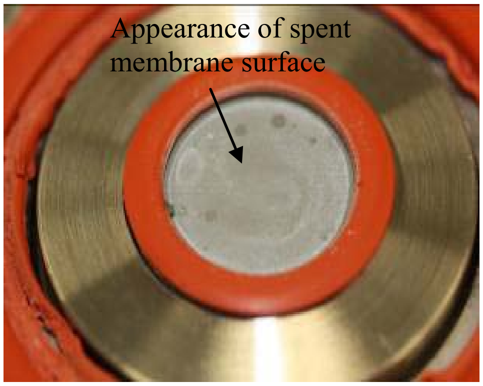

Figure 12. Morphology and structure of Cell 2 membrane sample (sheet 09/28/10 No.1) after long-term testing from January 14 to February 23, 2011.

A new membrane sheet was prepared and tested with the model and real feeds, and the results are summarized in Figures 13 and 14. Two membrane coupons were punched out of the same membrane sheet, and one each was loaded into Cell 1 and Cell 2 for testing. The two membranes were tested under similar conditions, enabling a check of the uniformity of the membrane sheet. The testing was started with a model feed comprising 90 wt% ethanol in water. No base was added, so pH was about 7. Then, the neutralized mixture of PEI#4 and PEI#5 was used as a feed. Finally, the membrane was retested with the model feed. Due to simple composition of the model feed, impacts of the real feed testing on the membrane structure can be assessed by comparing the separation results of the same membrane before and after exposure to the real feed in Figure 13. Figures 13a and 13b show that the two membrane coupons exhibit similar separation performances with the model feed, which indicates uniformity of this membrane sheet. By comparing Figure 13a to 13c for Cell 1, we can see that the permeation flux was lowered after the real feed testing. Figures 13b and 13d show that the permeation flux also decreased for Cell 2 after the real feed. The ethanol content in the permeate looks generally lower after the real feed testing than the initial run, which indicates improvement of the ethanol/water selectivity after the real feed testing.

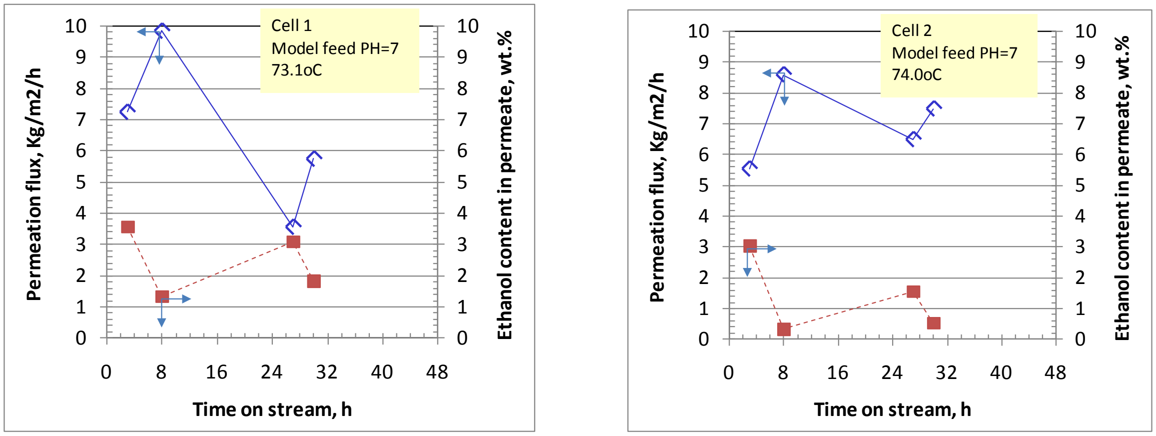

(a). Cell 1 – initial

(b). Cell 2 – initial

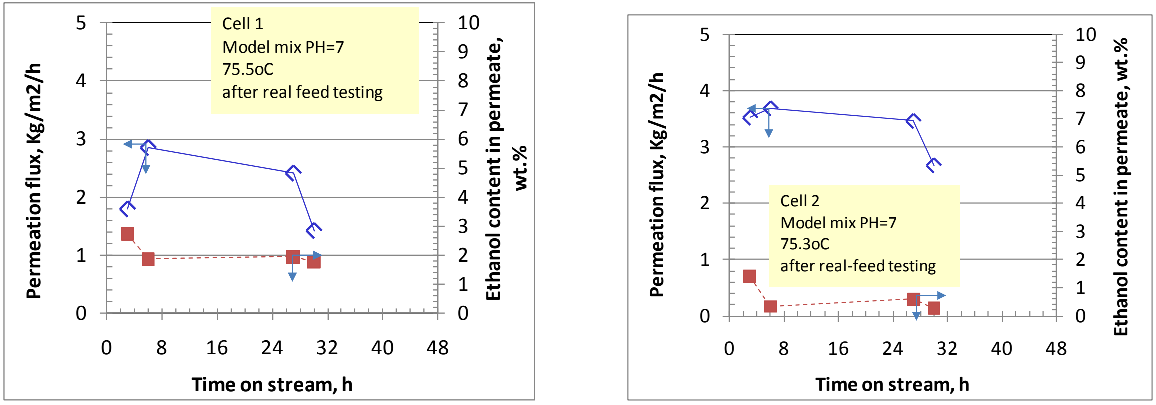

(c). Cell 1 –after real feed testing

(d). Cell 2 – after real feed testing

Figure 13. Change of membrane performances before and after real feed testing as measured with a model feed (NaA membrane 02/07/11 No.1 sheet, cell 1 and cell 2).

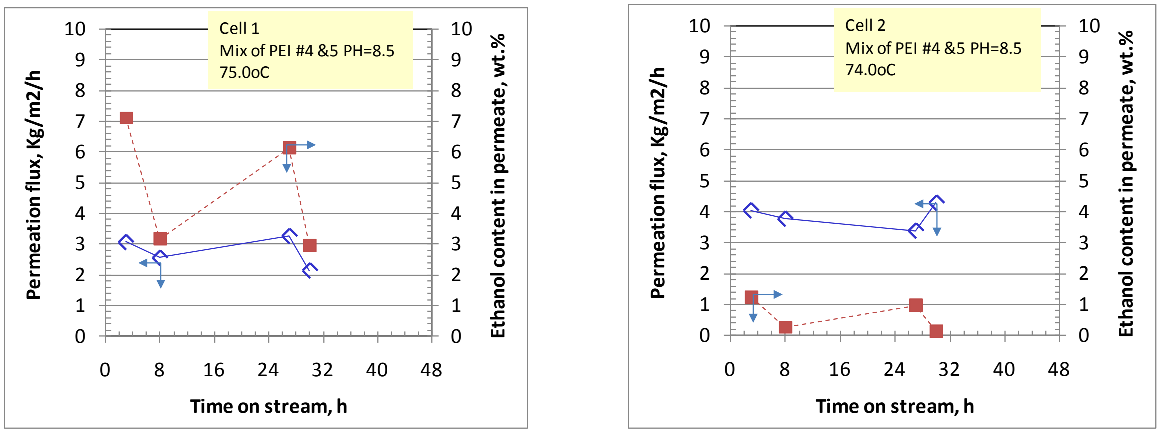

(a). Cell 1 – at 75.0 °C

(b). Cell 2 – at 74.0 °C

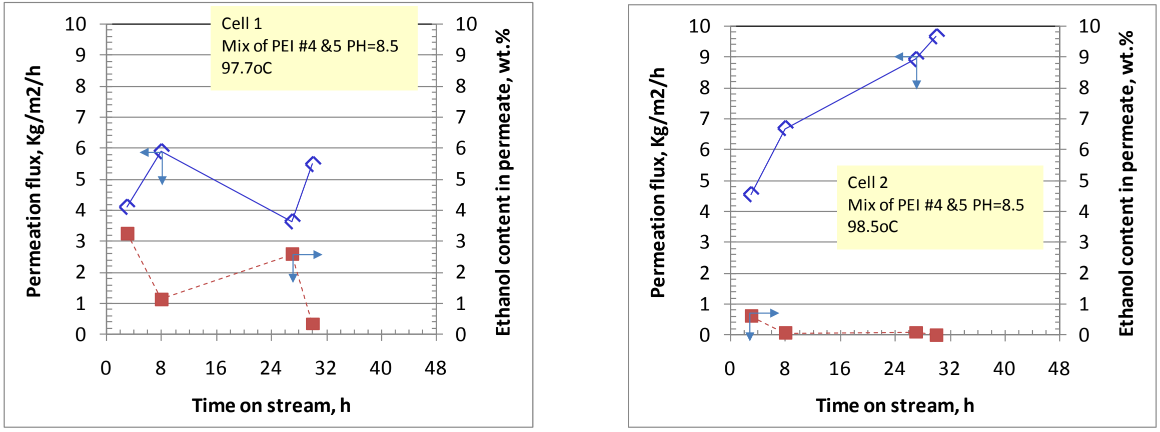

(c). Cell 1 – at 97.70 °C

(d). Cell 2 – at 98.5 °C

Figure 14. Membrane performances with neutralized mixture of PEI#4 and PEI#5 (the same test cells used as shown in Figure 13).

Testing results of the two membrane samples with the neutralized mixture of PEI#4 and PEI#5 are summarized in Figure 14. For both cells, the permeation flux and ethanol/water selectivity were enhanced by increasing the separation temperature from 167 °F to 208 °F (75 °C to 97.7 °C). The enhancements to both flux and selectivity may be contributed by increased water vapor pressure in the feed and in situ improvement of the membrane. The latter factor is particularly evident from the continuing increase of the permeation flux with time in Figure 14d.

It is clear that the real feed contains some components other than ethanol and water, which may react with the membrane under separation conditions. A guide bed can be installed to scrub the undesirable species prior to the feed stream entering into the membrane cells. Potential guide bed materials have been researched and several samples are acquired. Figures 15 and 16 show testing results obtained with two different guide bed materials. The real feed prepared by mixing PEI#4 and PEI#5 was used in these runs. Figure 15 shows an increase of ethanol content in the permeate and decrease of the permeation flux, which suggests probable degradation of the membrane by the real feed. However, this testing was aborted due to plugging of the guide bed. The separation performances with another guide bed material behave erratically, as shown in Figure 16. Post-test check of the membrane revealed that the fine particulate was entrained by the feed from the guide bed and deposited on the membrane surface. Thus, observed experimental results may be caused by mechanical artifacts in addition to the intrinsic membrane performance attributes. Further research and testing of suitable guide bed materials were pursued.

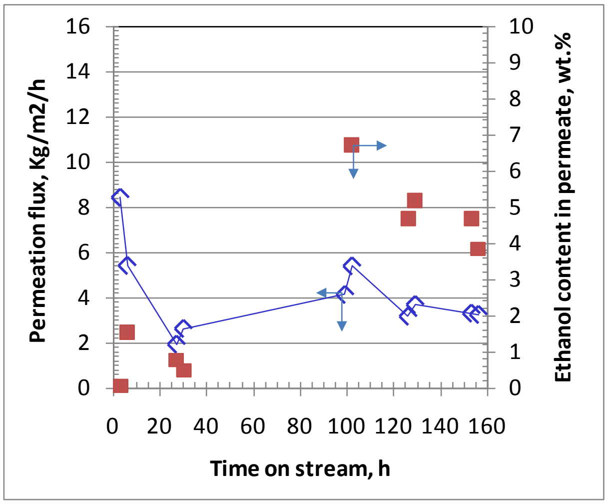

Figure 15. Impact of a guide bed on membrane separation performances with mixture of PEI#4 and PEI#5 as prepared (pH = 4.47) (guide bed material 1; Cell 2; NaA membrane 02/07/11 No.1 sheet; 110.7 °C).

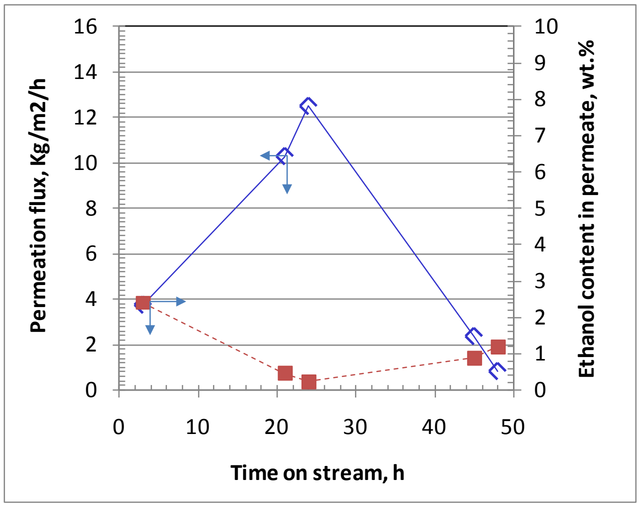

Figure 16. Impact of a guide bed on membrane separation performances with mixture of PEI#4 and PEI#5 as prepared (pH = 4.47) (guide bed material 2; Cell 2; NaA: membrane 03/01/11 No.1 sheet; 110.4°C).

3.3 Evaluation of Guide Bed Materials

From the earlier studies, it was concluded that the NaA membrane separation performance should be stable if the feedstock is free of acidic compounds. Thus, a series of adsorbent materials as listed in Table 3 was tested to identify efficient guard bed materials that enable long-term stable separation with the actual feedstock. The adsorbent is expected to remove or neutralize the acidic compounds present in the actual feedstock and thus prevent the membrane from degrading.

Table 3. Adsorbent materials evaluated

No.	Adsorbent name	Supplier
1	Amberlite IRA-458	Polyscience
2	Amberlite IRA-900	Polyscience
3	Amberlite IRA-93	Polyscience
4	Amberlite IRA-958	Polyscience
5	MgO	Aldrich
6	Type D-201 activated alumina 7 x 12 mesh beads	UOP
7	Type A-201 activated alumina 7 x 12 mesh beads	UOP
8	Type AW-300 molecular sieve, 1/16-in. pellets or beads	UOP
9	Type AW-500 molecular sieve, 1/16-in. pellets or beads	UOP

The stability of the adsorbent material was prescreened by following a procedure developed in our laboratory. Typically, a certain amount of adsorbent material was added into a real feedstock (a solution mixture of equal mass of PEI#4 and PEI#5), and the mixture was heated to 203 °F (95 ^{o}C) and held overnight. The solution pH was measured before and after contact with the adsorbent to check whether the acidity of feedstock was neutralized by the adsorbent. At the same time, the morphologies of the adsorbent after adsorption were visually examined to assess its structural integrity. The following adsorbents were selected from the screening test as a potential guard bed material and tested under ethanol/water separation conditions: MgO, Amberlite IRA-93, Amberlite IRA-958, and Amberlite IRA-458. The testing results are summarized in Table 4.

Table 4. Testing results of the membrane samples with real feedstock (feed flow rate = 3cc/min, feed pressure ~ 2 bar, feed =equal mass ratio of PEI#4 and PEI#5).

Membrane growth solution			Membrane testing conditions					
Number	Na	H_2O	Feed	Adsorbent	Temp (^{o}C)	Duration (hr)	Water flux (kg/m^2/hr)	Water/ethanol selectivity
051711_No.2	8	600	Model	-	110	32	1.9-8.2	33-760
020711_No.1	20	1500	Real	MgO	115	156	2.6-8.4	-
030111_No.1	20	1500	Real	IRA-93	112	48	12.7-13	36-632
030111_No.2	20	1500	Real	IRA-958	113	186	2.4-14.5	10-21
051711_No.1	8	600	Real	IRA-458	125	96	1-9.97	213-214
030111_No.3	20	1500	Model	IRA-958	95	80	3.3-7.1	132-488
031511_No.1	20	1500	Model	IRA-458	107	80	15.1-25.3	35-53
031511_No.4	20	1500	Model	-	112	72	2.4-4.7	857
031511_No.4	20	1500	Real	IRA-93	100	682	1-11	268-10342

Figure 17 shows the impact of different guard bed materials on membrane stability. The membrane samples associated with these tests are listed in Table 4. As shown in Figure 17, the water permeation dropped drastically with time when the IRA-958 and 458 were used as the guard bed materials, possibly due to the poor stability of these adsorbents under the separation testing conditions. With the MgO adsorbent particles, the permeation flux slightly decreased with time, which is expected due to decreased water content in the feed. However, the membrane lost its selectivity gradually. Post-test examination of the spent membrane showed deposition of fine MgO particles on the membrane surface, which may have caused the decline of membrane selectivity. The deposited MgO particles were possibly leached out of the guard bed. Compared to the other adsorbents, IRA-93 shows the most stable and effective performance that potentially enables a long-term separation with the real-world feedstock. As such, IRA-93 was identified as a candidate guard bed material for a long-term (> 500 hr) stability test.

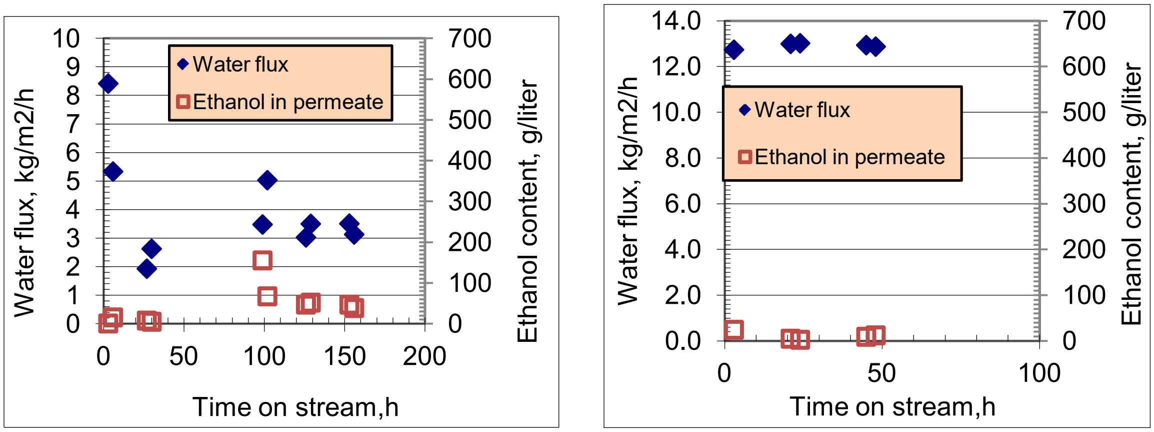

(a) MgO

(b) IRA-93

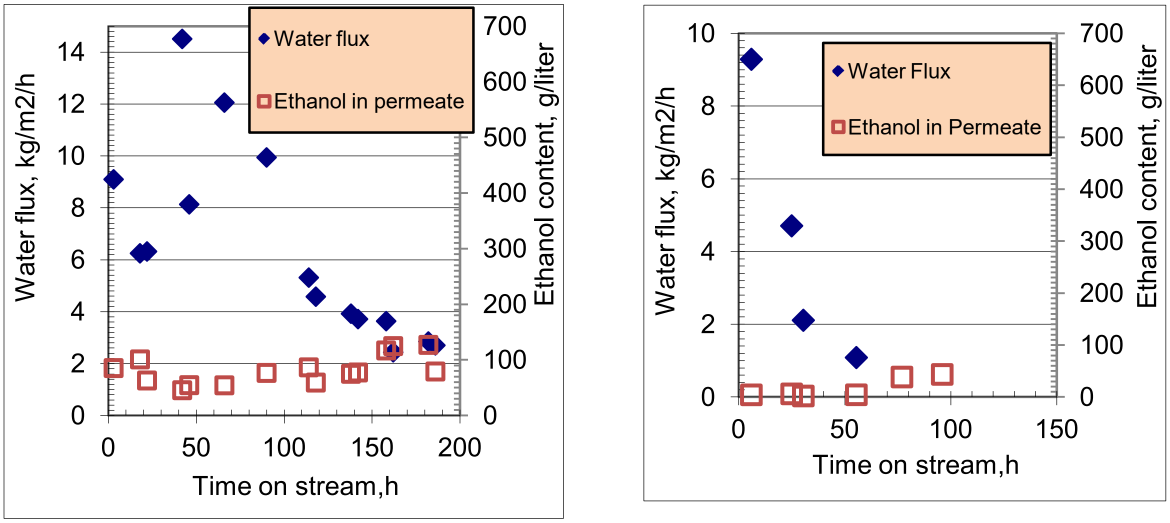

(c) IRA-958

(d) IRA-458

Figure 17. Stability testing of NaA membrane samples with the actual feed by using different guard bed materials.

Figure 18 shows the results of membrane 031511_No.4 with the IRA-93 guard bed material from a 700-hr stability test. The water permeation increased significantly from 4 kg/m^2/hr to 12 kg/m^2/hr when the feed was switched from the model to the actual feed due to the increased water content. The water permeation gradually decreased with time on stream due to the decreased driving force of partial pressure differential across the membrane. The feed tank was refilled with fresh feed after about 520 hr into the test; the water permeation increased but did not reach the value of 12 kg/m^2/hr. This suggests that the membrane stability slightly decreased with time. The ethanol content was kept low all the time, suggesting that the membrane did not lose its selectivity during a 700-hr run.

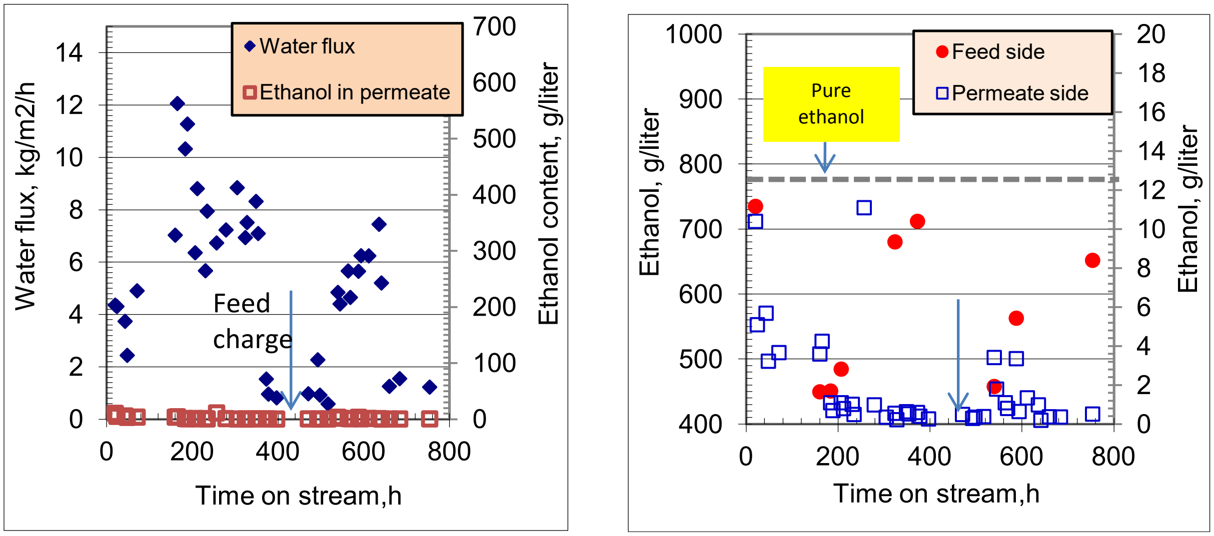

Figure 18. 700-hr stability testing of NaA membrane sample using IRA-93 guard bed material. The model feed was used for the first 96 hr, followed by the actual feed with feed tank refilling at about 96 hr and 520 hr.

The use of a guide bed enables long-term separation testing of the actual feed. Then we conducted sorption studies of the three resin sorbents listed in Table 5. Figure 19 shows the breakthrough curves of the real feed through respective guide beds. The highest sorption capacity was obtained with Amberlite IRA-93, which is consistent with the separation testing results described above. Compared to IRA-93, the other two sorbents lost their sorption capacity quickly, reaching 30% breakthrough at ~250 min for IRA-958 and at ~400 min for IRA-458.

Table 5. Characteristics of three resin sorbents used for the sorption study.

Name	Matrix	Matrix active group	Capacity (meq/g, dry basis)	Temperature Limit	Operating pH range
Amberlite IRA-93	Polystyrene	Polyfunctionality -NH; N	1.2 meq/mL	100 °C max.	0–9
Amberlite IRA-958	Acrylic copolymer (macroreticular)	quaternary ammonium functional group	0.8 meq/mL	79 °C max.	0–14
Amberlite IRA-458	Acrylic polymer (gel)	quaternary ammonium functional group	1.25 meq/mL	35 °C max.	0–14

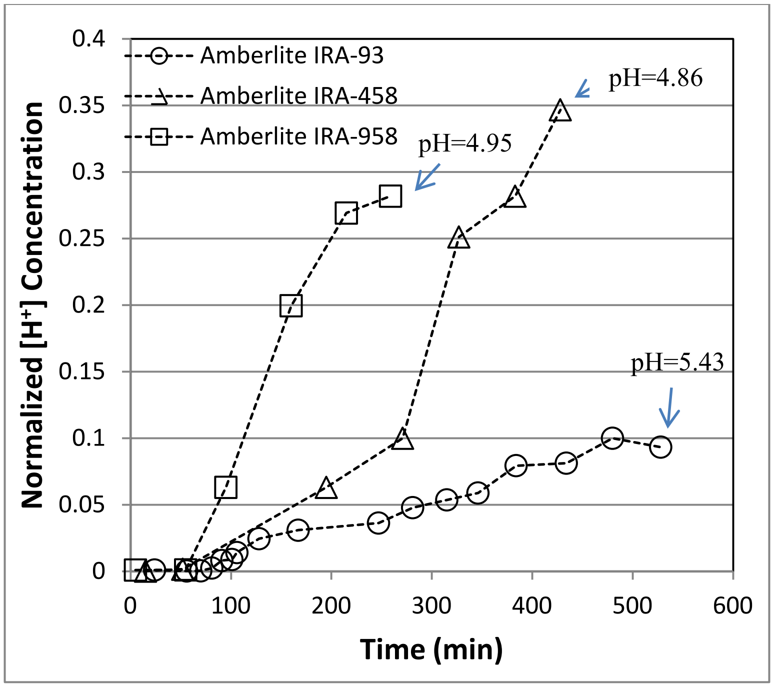

Figure 19. Comparison of breakthrough curves of a real feed through three resin sorbents (feed: equal weight ratio of PEI#4 and PEI#5 mixture; feed flow rate = 2 cc/min; test temperature: 98 °C; sorbent amount ~ 2.9 g).

The performance difference among different sorbents may be explained by the thermal stability of these materials under the testing conditions. As indicated in Table 5, our testing temperature was above the temperature limit of the original product specification. After the sorption test, we observed that all the sorbents maintained their round shape and sizes, i.e., mechanical integrity, but their colors changed. Fresh IRA-958 and IRA-458 were white powder, and both turned into dark brown after usage. IRA-93 slightly lost its original light-brown color. These observations suggest that the sorbents either had different degrees of degradation under the testing condition or absorbed some other species from the real feed.

We conducted SEM/EDS analysis of the membranes tested with the real feed to understand causes of the membrane performance change. Figure 20 shows the surface textures of two spent membrane samples (#030111_No.1 and #031511_No.4), which were tested for stability with IRA-93 as the guide bed sorbent in the previous quarter. For the spent membrane #030111_No.1, the membrane surface looks clean and the zeolite crystal is well preserved. The EDS analysis confirms that the membrane composition is consistent with that of NaA-type zeolite. Compared to the fresh membrane, a significant amount of C element was identified present on the membrane surface, which is possibly due to deposits of the biomass present in the real feed. For spent membrane #031511_No.4, the membrane surface was covered by some particles that contain Ca and C elements, which caused a deviation of the surface composition from the typical stoichiometric molar ratio of Al:Na:Si for NaA crystals. This membrane was tested for 700 hr. The result indicates that the guide bed may have no longer been effective in the late stage of testing. Thus, further stability studies with different guide bed designs and materials are necessary for membrane separation of the real feeds.

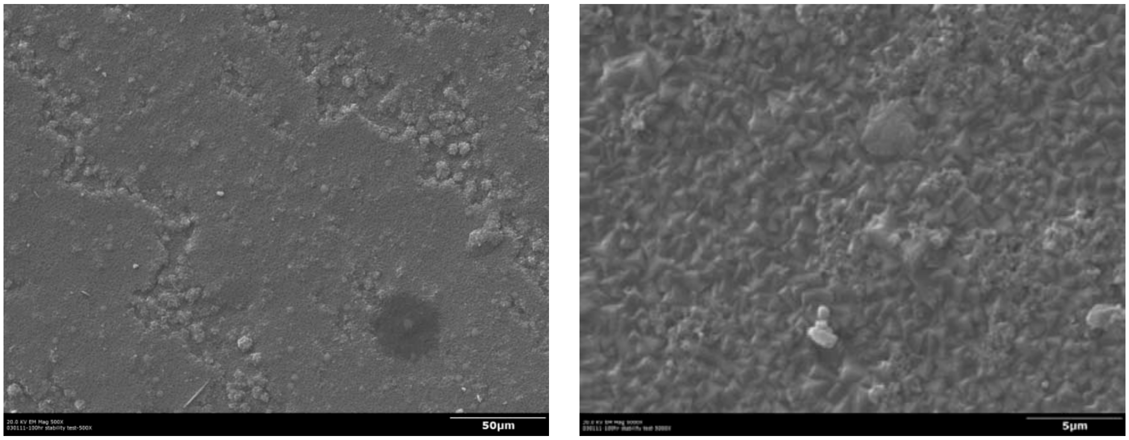

O	Na	Si	Al	C
45.1%	12.4%	15.6%	14.3%	11.7

O	Na	Si	Al	C
45.1%	11.8%	15.5%	14.2%	12.5

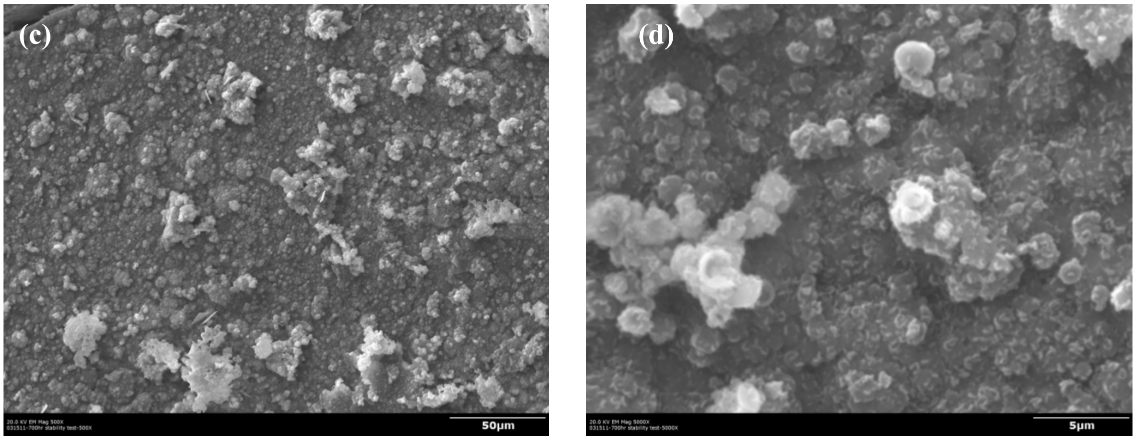

O	Na	Si	Al	Ca
40.5%	1.2%	15.2%	4.0%	3.6%

O	Na	Si	Al	Ca
46.3%	3.0%	18.7%	6.3%	4.9%

Figure 20. SEM/EDS analysis of two spent membrane samples (a) and (b) for 030111_No.1 after a 48-hr stability test; (c) and (d) for 031511-No.4 after a 700-hr stability test with the actual feed.

3.4 Analysis of Metal Content in Permeate

Based on a discussion between PNNL and Pacific Ethanol, alkaline metal ions such as Na^+ should not be present in the ethanol fuel product and in the processing water. The membrane separation tests suggested presence of reactive species other than water and ethanol in the real feed. Thus, elemental compositions of the real feeds and membrane separation samples were analyzed.

The composition of each sample after appropriate dilution was determined using the inductively coupled plasma/atomic emission spectrometry (ICP/AES) technique (Optima 7300DV, Perkin Elmer). Three emission lines were chosen for each element as a crosscheck for spectral interference. The calibration standards were matrix-matched in water, 10 mL of an original sample solution was taken into a glass vial, the glass vial without cap was placed in a hood overnight to allow organic solvent to evaporate completely, and then the residual was dissolved with a 2% nitric acid solution at a volume of 100 mL, a 10-fold dilution of the original solution. Table 6 lists analytical results of two process streams sampled from the Pacific Ethanol plant (PEI#4 and PEI#5). Indeed, presence of S in these two feeds is significant. The metal content in PEI#4 is much more than that in PEI#5, which is expected.

Table 6. Elemental analysis of real feed (units in ppm).

Sample ID#	Feed property		ICP/AES analysis			
	wt% ethanol	pH	K	Na	Ca	S
PEI#4	23.0	3.6	0.252	0.589	0.089	1.053
PEI#5	93.6	5.3	0.026	0.305	0.073	0.551

To understand distribution of metal elements after the membrane separation, we sampled the feed and permeate liquid at the beginning and end of each batch run. The analysis was conducted following the same procedure as described above. Tables 7 and 8 summarize the analytical results for two separate batch runs. Sample ID numbers starting with "F" and "P" represents the respective feed and permeate sample. The mixtures of PEI#4 and PEI#5 were neutralized by NaOH and KOH solution, respectively, in these two runs. Table 7 shows the significant presence of Na^+ and S^{++} in the feed samples in this run. In sharp contrast, the metal content in the permeate is about two to three orders of magnitude less than that in the corresponding feed. The result confirms the H_2O-selective permeation function of the NaA membrane material.

Table 8 shows that K^{++} content in the feed neutralized with KOH is significantly higher than the original K^{++} content, as expected. Consistent with the previous conclusion, permeation of metal elements across this H_2O-selective membrane is minimal. However, by comparing the metals in the feed and in the permeate, we can see that this NaA membrane seems more permeable to Na^+ than to K+. This is explained by larger K^+ ion size than Na^+.

Table 7. Elemental metal analysis of samples generated from membrane separation testing (feed: 1:1 ratio of PEI#4 and PEI#5 neutralized with NaOH to pH = 8.5; separation temperature of 95 °C).

Sampling information			Ethanol, g/L	ICP result, ppm		
ID#	Generation date and time			K	Na	S
F2064	12/7/2011	10:00am–1:00pm	637	0.399	9.36	1.58
P2064	12/7/2011	10:00am–1:00pm	0.092	0	0.014	0.016
F2069	12/9/2011	4:00pm–6:00pm	841	0.473	12.3	1.92
P2069	12/9/2011	4:00pm–6:00pm	0	0	0.063	0.004

Table 8. Elemental metal analysis of samples generated from membrane separation testing (feed: 1:1 ratio of PEI#4 and PEI#5 neutralized with KOH to pH = 8.5; separation temperature of 98 .°C)

Sampling information			Ethanol, g/L	ICP result, ppm		
ID#	Generation date and time			K	Na	S
F2070	1312011	1:10pm–4:10pm	618	10.9	3.37	1.26
P2070	1312011	1:10pm–4:10pm	4.21	0	0.074	0.017
F2074	2022011	1:10pm–4:10pm	523(a)	12.8	3.76	1.53
P2074	2022011	1:10pm–4:10pm	0.065	0.006	0.043	0.004

(a) Analytical result is questionable.

4.0 Process Design Simulation and Economics Analysis for Implementation of Membrane Separation in Ethanol Plants

The H_2O-selective membrane developed in this project may be implemented into the current ethanol fuel production process in various process configurations. A two-stage membrane separation process as outlined in Figure 21 is proposed based on experimental results and analysis of existing plant process flow diagrams.

The membrane module is used to treat the overhead stream of the beer column, replacing existing distillation and adsorption technologies. A guide bed is used to protect the membrane unit by removing acidic compounds and any other materials that could degrade the membrane. The first-stage membrane separator enriches the ethanol to about 95 wt% with the permeate side operated under rough vacuum (about 10 kPa). The second-stage membrane is used to produce 99.5 wt% ethanol by operating the permeate under a high degree of vacuum (such as 1.0 kPa). The second-stage permeate is compressed by vacuum pump #1 to mix with the first-stage permeate stream. The mixture (stream 7 in Figure 21) is cooled down to condense the water vapor into liquid water. The condensation pressure is controlled by vacuum pump #2. The condensed liquid can be discharged by water pump #3 for recycling.

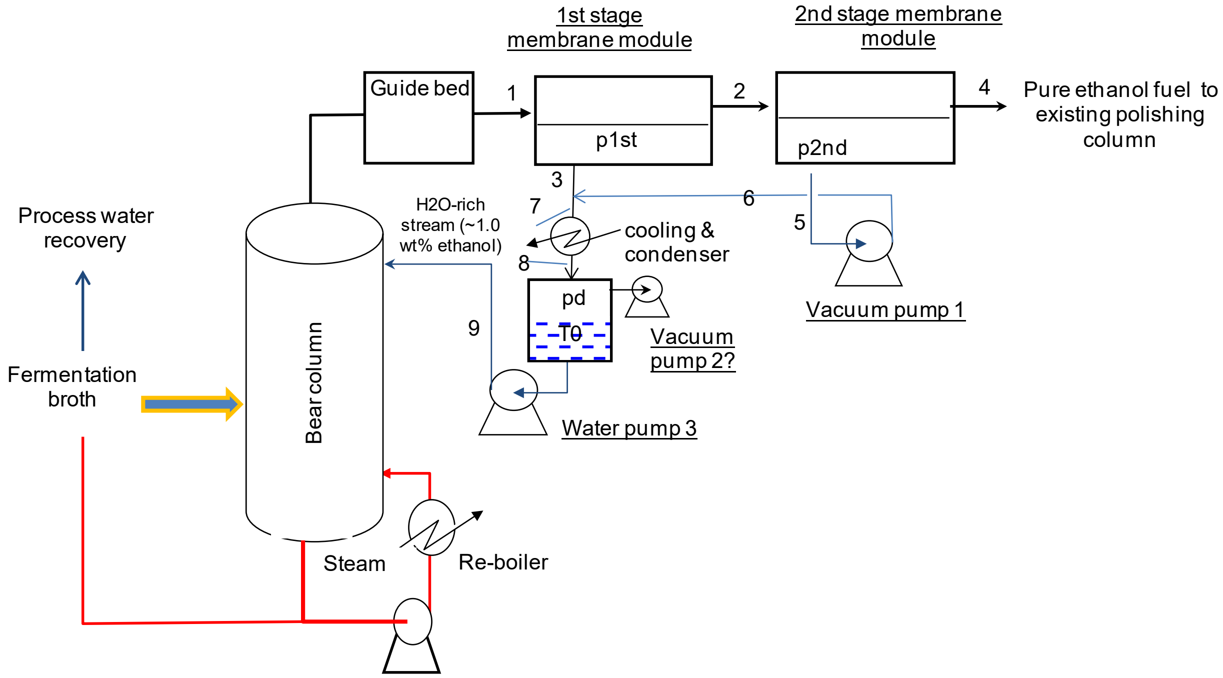

Figure 21. Simplified process flow diagram of two-stage membrane separator for production of pure ethanol fuel from overhead of beer column.

The ethanol/water separation mechanisms over the zeolite membrane can be complex. To simplify the calculation, the global permeance and separation factor are used to project the flux and permeate concentration, respectively.

$$P_1 = \frac{F_{1,P}}{SA_m \cdot \Delta p_1} \tag{1}$$

$$S_{12} = \frac{\left({}^{y_1}\!/\!{}_{y_2}\right)_P}{\left({}^{x_1}\!/\!{}_{y_2}\right)_F} \tag{2}$$

where

1 = water

2= ethanol

P_1 = permeance of water vapor, mol/m^2/s/Pa

S_{12} = separation factor of water to ethanol

SA_m = working surface area of membrane

$F_{1,P}$ = permeation flow rate of water, mol/s

Δp_1= average partial pressure differential of water vapor between the feed and permeate side

y_1= molar fraction of water in permeate

y_2 = molar fraction of ethanol in permeate

x_1 = molar fraction of water in feed

x_2 = molar fraction of ethanol in feed.

For a given feed composition, the permeate composition can be calculated from the separation factor:

$$y_1 = \frac{1}{1 + \frac{1}{S_{12}} \cdot \frac{1 - x_1}{x_1}} \tag{3}$$

An average partial pressure of water vapor is used to calculate the membrane area requirement for given feed and permeate conditions:

$$\Delta p_{1,avg} = \frac{\Delta p_{1,in} + \Delta p_{1,ex}}{2} \tag{4}$$

Isothermal compression is assumed to calculate power consumption of vacuum pumps for vapor compression:

$$w_{iso} = n_{vapor} RT \cdot Ln(\frac{P_{out}}{P_{in}}) \tag{5}$$

The following equation is used to calculate power consumption of the liquid pump:

$$w_{iso} = \Delta(P_{out} - P_{in}) \cdot V \tag{5}$$

Scope calculation of process streams and membrane sizes is conducted with the above equations. The results are summarized in Table 9. It can be seen that the membrane separation can be a very compact unit with first- and second-stage module sizes of only 3 and 1.5 m^3, respectively. The sizes are similar to those of a plate heat exchanger.

A USDA model was used to simulate the capital cost and energy consumption for a conventional dry corn mill plant that uses distillation and adsorption for enrichment and purification of ethanol. The results are tabulated in Tables 10 and 11. All the costs are based on 2007 cost indices. These results provide a comparative basis for the proposed membrane separation processes.

Three design cases are simulated to replace the distillation and/or adsorption process step with membrane separation. For membrane separation, condensation temperature of the permeate vapor is a critical process parameter that affects electrical power consumption of the vacuum pump. Figures 22 through 24 show the process diagrams for Cases 1, 2, and 3, respectively, while corresponding simulation results are summarized in Tables 12 through 17.

Table 9. Sizing of membrane separator for a 43-million gal/year ethanol plant.

Membrane performance			
Water permeance, mol/m^2/s/Pa	2.00E-06		
H_2O/ethanol separation factor	1.00E+02		
Membrane module feed - stream 1 (vapor)			
Total mass flow, kg/h	27,800		
Ethanol content, wt %	57.9%		
Pressure, kPa	180		
Temperature, K	373		
1st stage membrane module		**2nd stage of membrane module**	
Retentate - stream 2 (vapor)		**Retentate - stream 4 (vapor)**	
Pressure, kPa	160.0	Pressure, kPa	140.0
Water content, mol %	90.0%	Water content, mol %	99.0%
Water content, wt%	95.8%	Water content, wt%	99.6%
Flow rate, kmol/h	385.2	Flow rate, kmol/h	347.0
Permeate - stream 3 (vapor)		**Permeate - stream 5 (vapor)**	
pressure, kpa	6.24	pressure, kpa	1.00
Water content, mol %	99.5%	Water content, mol %	91.7%
Ethanol content, wt %	1.4%	Ethanol content, wt %	18.7 %
Flow rate, kmol/h	614.8	Flow rate, kmol/h	38.2
Membrane size		**Membrane size**	
Avg ΔP of water vapor, kPa	60.3	Avg ΔP of water vapor, kPa	7.8
Membrane area, m^2	1416	Membrane area, m^2	682
Packing density, m^2/m^3	500	Packing density, m^2/m^3	500.0
Module volume, m^3	2.8	Module volume, m^3	1.4
Membrane unit cost, \$/m^2	200	Membrane unit cost, \$/m^2	200.0
Total membrane cost, \$	\$283,232	Total membrane cost, \$	\$136,372

Table 10. Capital procurement cost of distillation and adsorption section in a conventional dry mill plant.

Molecular Sieve	\$1,717,700	From USDA model
Rectifier	\$142,600	
Regeneration/Ejector Liq Pump	\$4,100	
Stripper Col Reboiler	\$50,500	
Rectifier Btms Pump	\$6,000	
Stripper Tower	\$117,700	
Stripper Btms Pump	\$4,800	
Reflux Condenser	\$104,600	
Reflux Pump	\$6,800	
Total Bare Equipment	**\$2,154,800**	

Table 11. Energy consumption of distillation and adsorption section in a conventional dry mill plant.

Steam Consumption:	kg/hr	**Source**		
Molecular Sieve	182	Estimated from Chemcad model		
Stripper Reboiler	19,200			
1st Effect Evaporator	0	Uses heat removed from rectifier condenser, which has a higher flow rate than the ethanol product flow stream		
Total	**19,382**			
Electricity consumption	KW		Stream flow rate, kg/hr	
			USDA model	**Plant**
Molecular Sieve	13.7	Estimated from USDA model	14772	14081
Regen / Ejector Liquid Pump	1.1		4526	9552
Rectifer Bottoms Pump	5.5		18743	46451
Stripper Btms Pump	1.3		12929	11200
Reflux Pump	5.9		31915	51317
Total	**27.5**			

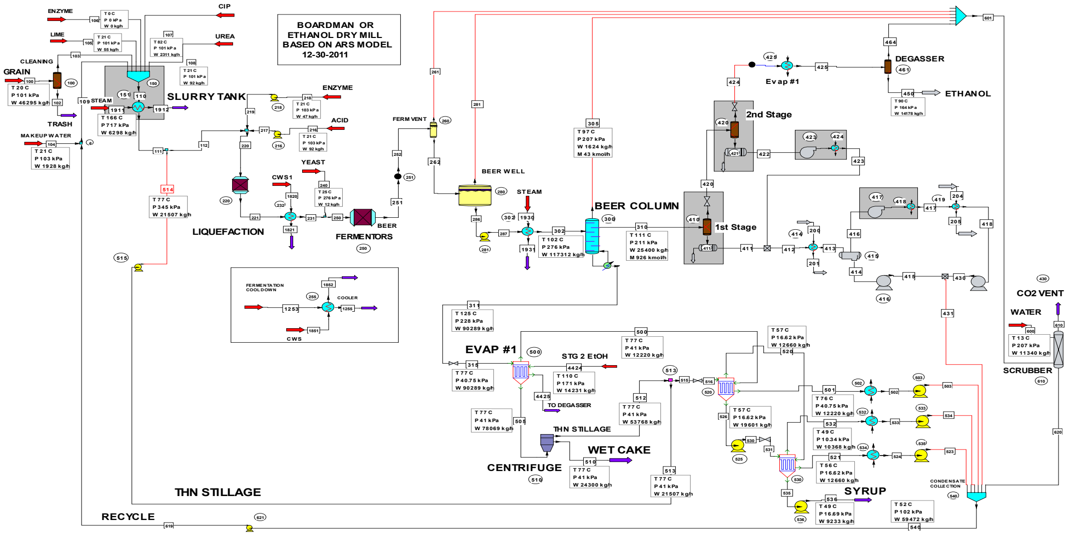

Figure 22. Process flow diagram for Case 1: two-stage membrane unit with cooling tower water.

Table 12. Capital cost of membrane system for Case 1.

Item	**Cost**	**Material**	**Source**
Membrane #1	$283,232	zeolite	Assumptions in Table 9
Membrane #2	$136,372	zeolite	
Vac Pump #1	$7,800	SS	From Aspen Capital Cost Estimator
Vac Pump #2	$18,900	SS	
Water Pump	$7,000	CS	
Condenser E414	$72,600	CS	
Condenser E419	$1,000	CS	
Unscheduled Equipment, 15%	$16,000	CS	
Initial Equipment	**$542,904**		
Membrane life, yr	1.6		
Plant life, yr	20		
Replacement Membrane Cost	$1,568,278		
Total Equipment	**$2,111,182**		

Table 13. Energy consumption of membrane system for Case 1.

Steam	kg/hr	**Source**
First Effect Evaporator	0	Use heat from stage 2 membrane ethanol cooler and readjust evaporator load
Total	**0**	
Electrical	kW	
Vacuum Pump #1	20	Chemcad model - rough estimate, model needs additional detail
Vacuum Pump #2	84	
Misc. Liquid Pumps	0.4	
Total	**104.4**	

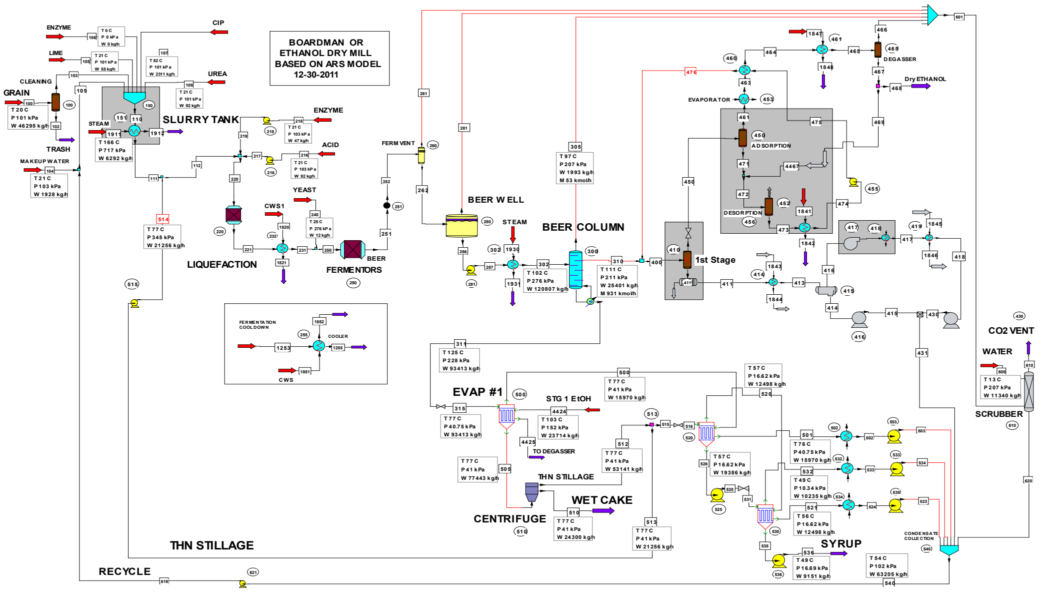

Figure 23. Process flow diagram for Case 2: single-stage membrane unit with conventional molecular sieve for product finishing.

Table 14. Capital cost of membrane system for Case 2.

Item	**Cost**	**Material**	**Source**
Membrane #1	$283,232	zeolite	Table 9
Molecular Sieve	$1,717,700		from USDA Model
Vac Pump #1	$7,800	SS	From Aspen Capital Cost Estimator
Water Pump	$7,000	CS	
Condenser E414	$72,600	CS	
Unscheduled Equipment, 15%	$13,000	CS	
Initial Equipment	**$2,101,332**		
Membrane life	*20*		
Plant life	20		
Replacement Membrane Cost	$0		
Total Equipment	**$2,101,332**		

Table 15. Energy consumption of membrane system for Case 2.

Steam	kg/hr	**Source**
1st Effect Evaporator	0	Use heat from stage 2 membrane ethanol cooler and readjust evaporator load
Molecular Sieve	182	Estimated from Chemcad model
Total	**182**	
Electrical	kW	
Vacuum Pump #1	20	Chemcad model - rough estimate, model needs additional detail
Mol Sieve	13.7	Estimated from USDA model
Regen / Ejector Liquid Pump	1.1	
Misc. Liquid Pumps	0.4	Chemcad model - rough estimate
Total	**35.2**	

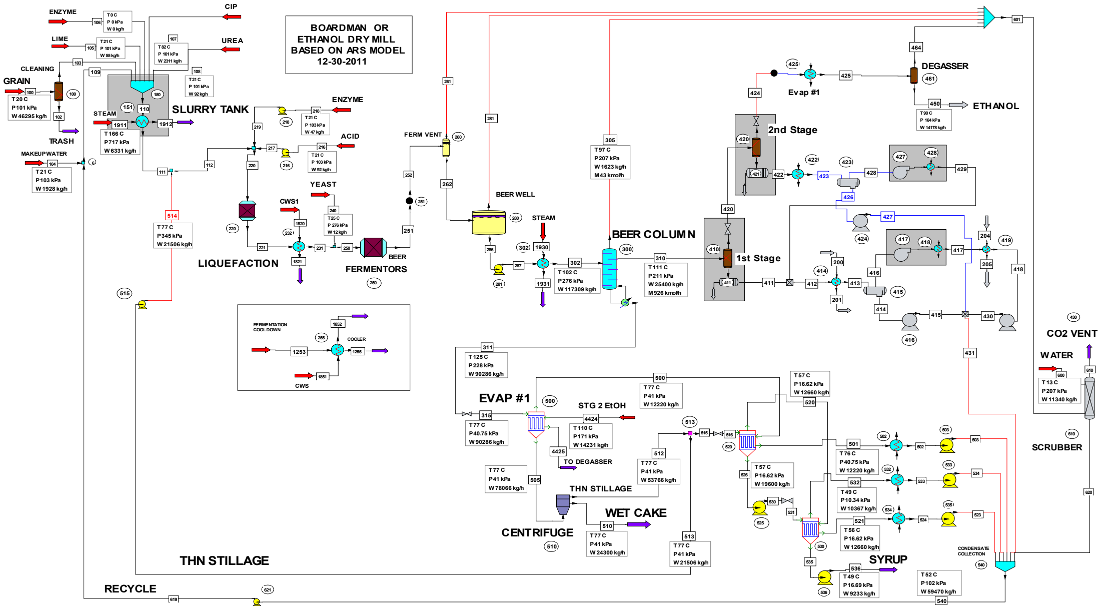

Figure 24. Process flow diagram for Case 3: two-stage membrane unit with cooling tower water and well water available.

Table 16. Capital cost of membrane system for Case 3.

Item	Cost	Material	Source
Membrane #1	$283,232	zeolite	Table 9
Membrane #2	$136,372	zeolite	
Vac Pump #1	$7,800	SS	From Aspen Capital Cost Estimator
Vac Pump #2	$18,900	SS	
Water Pump	$7,000	CS	
Condenser E414	$72,600	CS	
Condenser E419	$1,000	CS	
Unscheduled Equipment, 20%	$21,000	CS	
Initial Equipment	**$547,904**		
Membrane life	1.6		
Plant life	20		
Replacement Membrane Cost	$1,568,278		
Total Equipment	**$2,116,182**		

Table 17. Energy consumption of membrane system for Case 3.

Steam	Kg/h	**Source**
1st Effect Evaporator	0	Use heat from Stg 2 membrane ethanol cooler and readjust evaporator load
Total	**0**	
Electrical	kw	
Vacuum Pump #1	19.4	Chemcad model - rough estimate, model needs additional detail
Vacuum Pump #2	6.4	
Misc. Liquid Pumps	0.4	
Total	**26.2**	

Energy consumption and capital costs of three membrane-modified plant designs are compared to the existing plant in Table 18. For an existing plant, steam usage dominates the energy consumption. For two-stage membrane separation (Cases 1 and 3), steam consumption is nearly zero, and electrical power consumption is heavily dependent on the temperature of cooling water used to condense permeate water vapor. Because the electrical power consumption in membrane separation is due primarily to the vacuum pumps, the power consumption dramatically decreases with decreasing cooling water temperature. If only one-stage membrane separation is used to replace the distillation column only (Case 2), there is steam consumption to run the adsorption process. Overall energy consumption of the membrane separation is very small relative to existing distillation and adsorption processes, and greater than 90% energy savings is shown.

Table 18. Comparison of energy consumption and capital costs for ethanol enrichment and purification (40 million gal/year of ethanol).

	Case 1: Two-stage membrane with cooling tower water only	Case 2: One-stage membrane with a molecular sieve	Case 3: Two-stage membrane with well water available
Energy consumption			
Existing plant with distillation and adsorption			
Steam, kg/hr	19,382	19,382	19,382
Electrical, kW	27	27	27
Total[a], kW	14,816	14,816	14,816
Modified plant with membrane separation			
Steam, kg/hr	0	182	0
Electrical, kW	104	35	26
Total[a], kW	334	294	84
Reduction %	97.7%	98.3%	99.4%
Capital cost			
Existing plant, $	$2,154,800	$2,154,800	$2,154,800
Plant life, year	20	20	20
Modified plant with membrane separation			
Initial equipment, $	$542,904	$2,101,332	$547,904
Membrane life required, year	1.6	20	1.6
Plant life, year	20	20	20
Replacement membrane cost, $	$1,568,278	$0	$1,568,278
Total equipment, $	$2,111,182	$2,101,332	$2,116,182
(a) Electrical energy is converted into thermal energy using a factor of 3.2. Thermal energy of steam is calculated as 0.76 kW/(kg/hr).			

Capital costs are compared on the basis of a 20-year plant lifetime for existing distillation and adsorption equipment. This is a big assumption because the adsorbent lifetime may not last that long. For Cases 1 and 3, the membrane lifetime needs to be 1.6 years to make the capital cost comparable to the existing cost. Obviously, the capital cost will be decreased with increasing membrane lifetime. For Case 2, a 20-year membrane lifetime (same as the assumed adsorbent material lifetime in the existing plant) is needed for the membrane plant cost to be comparable to the existing plant cost. The capital cost of the existing plant is due mainly to the adsorption separation process. Thus, using two-stage membrane separation to replace both distillation and adsorption process units is necessary to reduce the capital cost.

It is noted that the capital costs are compared here based on the equipment and material only. Actual installation cost can be a few times that of the equipment cost. Due to compactness of membrane separation modules, the major savings in the capital cost may result from savings of installation cost, which is not quantified in this work.

5.0 Conclusions

The following conclusions can be drawn from this research:

- NaA-type zeolite membranes degrade under separation conditions with as-received real feeds, although they are stable with model feeds made of pure ethanol and water.
- The zeolite membrane is stable under practical separation conditions with the real-world feeds after the acidic compounds in the as-received samples are neutralized with alkaline hydroxide or scrubbed using a guide bed.
- Defective zeolite membranes may be cured under separation conditions with a feed containing alkaline hydroxide.
- A two-stage membrane pervaporation process is proposed for removal of remaining water from overhead stream of the beer column. Compared to existing distillation and adsorption technologies, the membrane separation does not need steam and results in more than 90% energy reduction. This energy saving is equivalent to 9,924 Btu/gal of ethanol fuel.
- The membrane separation unit can be very compact due to high water permeation flux. For a 40-million gal/year plant, the two-stage membrane modules are estimated to be 3.0 and 1.5 m^3, which are comparable to the plate heat exchangers.
- The largest capital cost saving with the two-stage membrane separation process would likely result from installation, due to the compactness and simplified process flow diagram of the membrane unit. For the procurement cost of overall capital equipment to be comparable to the current distillation and adsorption section, the membrane needs to have a life time more than 1.6 years at a membrane unit cost of $200/$m^2$ with current permeance level demonstrated (2 $x10^{-6}$ mol/m^2/s/Pa).
- The membrane cost proportionally decreases with increasing membrane lifetime and permeance. Thus, building membrane module prototypes and demonstrating their long-term performances (permeance & lifetime) with slip streams in an ethanol plant are necessary to move the technology toward commercialization.

6.0 Intellectual Property and Documentation

Invention disclosure:

1. Liu W. "Membrane Separation Process for Ethanol Fuel Production." PNNL Invention Disclosure #IDR 16902-E.

7.0 Cited References

Liu W. 2012. *High-Surface-Area Inorganic Membrane for Process Water Removal*. PNNL-21139, Pacific Northwest National Laboratory, Richland, Washington.

Zhang J and W Liu. 2011. Thin porous metal sheet-supported NaA zeolite membrane for water/ethanol separation. *Journal of Membrane Science* 371: 197–210.

Liu W, J Zhang, N Canfield, and L Saraf. 2011. Preparation of robust, thin zeolite membrane sheet for molecular separation. *Industrial & Engineering Chemical Research* 50(20):11677–11689.

Liu W and N Canfield. 2012. Thin porous metal sheets as micro-filtration membrane and inorganic membrane support. *Journal of Membrane Science* 409-410:113–126.

Pacific Northwest
NATIONAL LABORATORY

U.S. DEPARTMENT OF
ENERGY

Proudly Operated by Battelle *Since 1965*

902 Battelle Boulevard
P.O. Box 999
Richland, WA 99352
1-888-375-PNNL (7665)
www.pnnl.gov